Published in final edited form as:
Toxicol Appl Pharmacol. 2011 November 1; 256(3): 227–240. doi:10.1016/j.taap.2011.07.018.

Manganese Nanoparticle Activates Mitochondrial Dependent Apoptotic Signaling and Autophagy in Dopaminergic Neuronal Cells

Hilary Afeseh Ngwa[a], **Arthi Kanthasamy**[a], **Yan Gu**[b], **Ning Fang**[b], **Vellareddy Anantharam**[a], and **Anumantha G. Kanthasamy**[a,*]

[a]Department of Biomedical Sciences, Iowa Center for Advanced Neurotoxicology, Iowa State University, Ames, IA, 50011, USA

[b]Department of Chemistry, Iowa State University, Ames, IA, 50011, USA

Abstract

The production of man-made nanoparticles for various modern applications has increased exponentially in recent years, but the potential health effects of most nanoparticles are not well characterized. Unfortunately, *in vitro* nanoparticle toxicity studies are extremely limited by yet unresolved problems relating to dosimetry. In the present study, we systematically characterized manganese (Mn) nanoparticle sizes and examined the nanoparticle-induced oxidative signaling in dopaminergic neuronal cells. Differential interference contrast (DIC) microscopy and transmission electron microscopy (TEM) studies revealed that Mn nanoparticles range in size from single nanoparticles (~25 nM) to larger agglomerates when in treatment media. Manganese nanoparticles were effectively internalized in N27 dopaminergic neuronal cells, and they induced a time-dependent upregulation of the transporter protein transferrin. Exposure to 25–400 μg/mL Mn nanoparticles induced cell death in a time- and dose-dependent manner. Mn nanoparticles also significantly increased ROS, accompanied by a caspase-mediated proteolytic cleavage of proapoptotic protein kinase Cδ (PKCδ), as well as activation loop phosphorylation. Blocking Mn nanoparticle-induced ROS failed to protect against the neurotoxic effects, suggesting the involvement of other pathways. Further mechanistic studies revealed changes in Beclin1 and LC3, indicating that Mn nanoparticles induce autophagy. Primary mesencephalic neuron exposure to Mn nanoparticles induced loss of TH positive dopaminergic neurons and neuronal processes. Collectively, our results suggest that Mn nanoparticles effectively enter dopaminergic neuronal cells and exert neurotoxic effects by activating an apoptotic signaling pathway and autophagy, emphasizing the need for assessing possible health risks associated with an increased use of Mn nanoparticles in modern applications.

Keywords

manganese; metals; nanoparticles; neurotoxicity; oxidative stress; nanotoxicology; autophagy; risk assessment; Parkinson's disease

*Corresponding author: Dr. Anumantha G. Kanthasamy, Parkinson's Disorder Research Laboratory, Iowa Center for Advanced Neurotoxicology, Department of Biomedical Sciences, 2062 Veterinary Medicine Building, Iowa State University, Ames, IA 50011, USA. Phone: +1-515-294-2516; Fax: +1-515-294-2315; akanthas@iastate.edu.

Introduction

Improved synthesis and characterization of nanoscale materials provide new opportunities for manufacture of never-before-seen materials. Particles ranging between 1 to 100 nm with unique size-dependent properties are now available for new, improved applications in an enormously wide range of technologies (Auffan, 2009). Over the last decade, the National Nanotechnology Initiative (NNI) has played a pivotal role in positioning the United States as the world leader in nanotechnology research, development and commercialization; approximately $12 billion in federal spending has been invested over the last decade (The President's Council of Advisors on Science and Technology, (2010). Nanomaterials receive attention for their use and applicability in the creation of new consumer products, and also for their ability to advance science with novel analytical tools that are relevant to both physical and life sciences (Cui and Gao, 2003; Wu and Bruchez, 2004; Hussain *et al*., 2006). A recent estimate suggests that more than 1,000 nanoparticle-containing consumer products are currently on the market (The Project on Emerging Nanotechnologies Consumer Products Inventory, 2011), with over $147 billion in product sales in 2007 (Nanomaterials state of the market Q3, (2008). The increased number of man-made nanoparticle products from large-yield industry production settings has increased the probability of human exposure throughout the life span. Despite the prevalence of newly engineered nanomaterials, there is still relatively little known about their potential impacts on human and environmental health (Marquis *et al*., 2009). Research efforts to assess the toxic potential of nanomaterials have presented some serious and far-reaching challenges, which have been addressed previously by several review papers (Balshaw *et al*., 2005; Holsapple *et al*., 2005; Thomas and Sayre, 2005; Borm *et al*., 2006; Thomas *et al*., 2006; Tsuji *et al*., 2006; Warheit *et al*., 2007). Limited studies have attempted to assess and characterize the toxicity of man-made nanomaterials (Lam *et al*., 2004; Oberdorster, 2004; Braydich-Stolle *et al*., 2005; Hussain *et al*., 2005; Monteiro-Riviere *et al*., 2005; Nel *et al*., 2006), but there remains an urgent need for well-designed studies that will generate data so that risk assessments for nanomaterials can be conducted.

Manganese is used in industrial applications involving steel and non-steel alloy production, colorants, battery manufacture, catalysts, pigments, fuel additives, ferrites, welding fluxes, and metal coatings (Han *et al*., 2005). With the advent of nanoparticle development, traditional macro-sized manganese particles will likely be replaced with Mn nanoparticles. For example, applications of Mn nanomaterials are currently being pursued for catalysis and battery technologies (Han *et al*., 2005). New industrial uses of Mn nanomaterials in both metallurgic and chemical sectors are therefore anticipated. Thus, the potential neurotoxic effects of these applications are not well characterized. With increasing evidence suggesting a link between Mn and neurotoxicity in humans (Aschner *et al*., 2006; Guilarte, 2010), particularly the etiopathogenesis of PD, research on emerging Mn nanoparticle technologies is urgently needed.

Manganese (Mn) is an essential element required in low microgram quantities for proper function. However, excessive and chronic exposure to manganese causes an irreversible brain disease with distinct PD-like psychological and neurological disturbances known as manganism (Aschner *et al*., 2006; Guilarte, 2010). Manganese exposure has been shown to produce neurotoxicity *in vitro* in dopaminergic cell culture models, and *ex vivo* and *in vivo* in animal models (Kitazawa *et al*., 2003; Jayakumar *et al*., 2004; Aschner *et al*., 2005; Latchoumycandane *et al*., 2005; Zhang *et al*., 2011). These studies provide evidence that Mn targets the dopaminergic system (Park *et al*., 2006; Zhang *et al*., 2011). Studies in humans indicate that elevated levels of Mn may, in fact, put humans at risk of parkinsonism (Olanow, 2004). In terms of mechanisms, Mn has been shown to cause cell death in dopaminergic neuronal cells by promoting oxidative stress and apoptosis (Kanthasamy *et*

al., 2003b; Kaul *et al*., 2003a; Kitazawa *et al*., 2003; HaMai and Bondy, 2004; Latchoumycandane *et al*., 2005; Afeseh Ngwa *et al*., 2009). Our laboratory has reported that increased oxidative stress and subsequent caspase-3-dependent activation of PKCδ by proteolysis are pivotal in manganese- and vanadium-induced oxidative damage in dopaminergic cell death (Kitazawa *et al*., 2002; Kitazawa *et al*., 2005; Latchoumycandane *et al*., 2005; Afeseh Ngwa *et al*., 2009; Kanthasamy *et al*., 2010). In addition to apoptosis, autophagy is emerging as an important mechanism underlying degenerative processes in dopaminergic neurons (Anglade *et al*., 1997; Kanthasamy *et al*., 2006; Cheung and Ip, 2009). In view of the anticipated increased environmental exposure to Mn nanoparticles resulting from increased nanoparticle applications, the neurotoxicological mechanisms must be vigorously investigated. Therefore, in the present study, we have characterized the uptake and neurotoxic mechanisms of manganese nanoparticles in cell culture models of Parkinson's disease.

Materials and Methods

Chemicals

We are grateful to QuantumSphere, Inc. (Santa Ana, CA) for supplying the nanoparticles used in this study. Sytox green nucleic dye was purchased from Molecular Probes (Eugene, OR). Z-Asp-Glu-Val-Asp-fluoromethyl ketone (Z-DEVD-FMK) and Z-VAD-FMK (Z-Val-Ala-Asp-fluoromethyl ketone) were purchased from Alexis Biochemicals (San Diego, CA). The Bradford protein assay kit was purchased from Bio-Rad Laboratories (Hercules, CA). RPMI 1640, B27 supplement, fetal bovine serum, L-glutamine, penicillin, and streptomycin were purchased from Invitrogen (Gaithersburg, MD). Protease cocktail, phosphatase inhibitors, and anti-β-actin antibody were obtained from Sigma-Aldrich (St. Louis, MO); mouse tyrosine hydroxylase (TH) was purchased from Millipore (Billerica, MA), rabbit transferrin (Tf), rabbit Beclin1, and rabbit PKCδ antibody were purchased from Santa Cruz Biotechnology, Inc. (Santa Cruz, CA); rabbit LC3 antibody was purchased from Abcam, anti-mouse and anti-rabbit secondary antibodies (Alexa Flour 680 conjugated anti-mouse IgG and rabbit IgG IR800 Conjugate) were purchased from Invitrogen and Rockland Inc., respectively.

Plasmid constructs

Dr. Isei Tanida of the National Institute of Infectious Disease, Japan, generously donated the GFP-LC3 and GFP-LC3-ΔG constructs. GFP-LC3-ΔG is a mutant, with a deleted C-terminal glycine essential for lipidation used as a negative control, to identify the lipidation-independent LC3 puncta.

Characterization of Mn nanoparticles by TEM (Transmission Electron Microscopy) and DIC (Differential Interferance Contrast) microscopy

TEM characterization was performed in the Microscopy and Nanoimaging facility at the office of Biotechnology at Iowa State University. Mn nanoparticles were examined after suspension in N27 cell culture treatment media. The concentration was 20 mg/mL. Mn nanoparticle size was measured using software for the digital TEM camera after appropriate calibration. Nanoparticle size was calculated from random field views with images that show single and agglomerated nanoparticles with their general morphology in the RPMI media (Fig. 1). Nanoparticle size was also estimated using a DIC method recently described in our publication (Sun *et al*., 2008). Briefly, DIC microscopy works on the principle of interferometry to gain information about the optical density of the sample. This is accomplished by illuminating a specimen with two orthogonally polarized light beams that are split by a Nomarski prism from a plane-polarized beam. A refractive index difference between the sample and its surrounding medium causes a phase difference for the passing

beams, which are recombined into a single beam by a second Nomarski prism to generate an interference pattern, thus revealing cellular features that cannot be seen under standard white light illumination. Particle sizes were calculated by measuring the pixels of the image and then estimating particle sizes. For example, one of the particle agglomerates observed on the screen was 20 pixels in diameter, 1.4 magnification, and each pixel is 45.6nm long, so the true diameter of that particle should be 20 × 45.6 nm=912 nm. The nanoparticles observed ranged in size from single nanoparticles (Fig. 1A) as small as ~ 25 nm to agglomerates (Fig. 1B) of up to ~ 900 nm.

Cell culture models and treatment

We used a dopaminergic neuronal cell line and mouse primary mesencephalic neuronal cultures in this study. A rat mesencephalic dopaminergic cell line, generally referred to as N27 dopaminergic cells, was a generous donation from Dr. Kedar N. Prasad (University of Colorado Health Sciences Center, Denver, CO). Our lab and other research groups have used N27 cells extensively to study the neurotoxic mechanisms related to Parkinson's disease (Clarkson *et al*., 1999; Miranda *et al*., 2004; Kaul *et al*., 2005; Peng *et al*., 2005; Kanthasamy *et al*., 2006). N27 cells were grown and exposed to appropriate concentrations of nanoparticles in RPMI 1640 medium supplemented with 10% fetal bovine serum, 2 mM L-glutamine, 50 units of penicillin, and 50 μg/ml of streptomycin in a humidified atmosphere of 5% CO_2 at 37°C, as described previously (Kaul *et al*., 2003a; Yang *et al*., 2004; Afeseh Ngwa *et al*., 2009). N27 cells were exposed to different concentrations of Mn nanoparticles for the duration of the experiments. Following exposure, cells were collected by trypsinization or scraping, spun down at 200 g for 5 min, and washed with ice-cold phosphate-buffered saline (PBS). The lysates from the cell pellets were appropriately used for various assays. For antioxidant studies, N27 cells were exposed to the treatments in RPMI 1640 medium supplemented with 2% B27 supplement with or without antioxidants instead of 10% fetal bovine serum (Afeseh *et al*., 2009).

Primary mesencephalic neuronal cultures were prepared from the ventral mesencephalon of gestational 14- to 16-day-old mouse embryos, as described in our previous publications (Yang *et al*., 2004; Sun *et al*., 2006; Afeseh Ngwa *et al*., 2009). Mesencephalic tissues from E14 to 16 mouse embryos were dissected and maintained in ice-cold DMEM solution supplemented with penicillin and L-glutamine, and then dissociated in Hanks' balanced salt solution containing trypsin-0.25% EDTA for 20 min at 37°C. Equal densities (0.7×10^6 cells) of the dissociated cells were then plated on coverslips in 24-well plates precoated with 1 mg/ml poly-D-lysine. The cultures were maintained in neurobasal medium supplemented with B-27 supplements, 500 μM L-glutamine, 100 IU/ml penicillin, and 100 μg/ml streptomycin (Invitrogen, Carlsbad, CA). The cells were grown in a humidified CO_2 incubator (5% CO_2 and 37°C) for 24 h. Half the volume of the culture medium was replaced every 2 days. Approximately 5- to 7-day-old cultures were used for experiments. Primary mesencephalic dopaminergic neuronal cells were exposed to appropriate concentrations of Mn nanoparticles, and following exposure, the cells were fixed and stained for TH.

Dosimetry

Doses of nanoparticles in an *in vitro* system are more difficult to meaure and more difficult to compare across particle types than chemical doses. Nanoparticles are affected by their solution dynamics, in that they can diffuse, settle, agglomerate, and change surface charge/chemistry over time in solution, changing the nature of the particles and their transport to cells depending on the exposure conditions. The solution dynamics are in turn affected by the intrinsic properties of the particles themselves, e.g., size, density, and surface chemistry, as well as the solution (viscosity, density, presence of proteins, etc.). Particles of different sizes and densities, for example, settle at different rates. These differences might correspond

to differences in transport to, access and entry into cells in culture. To date, the full extent of these differences and their impact on the toxicity assessment, as far as particles in general and nanoparticles in particular are concerned, are still scantily understood and widely unappreciated (Teeguarden *et al*., 2007).

The volume of the desired concentration of Mn nanoparticles for experiments in this study seeded into well plates or flasks was calculated based on the surface area relationship between the flasks/well plate. This was done to ensure delivery of the same number of nanoparticles per unit area across treatments in experiments. For all experiments where the calculated volume exceeded the carrying capacity of the flask/well, the volume was reduced and the concentration was appropriately adjusted to ensure the same numbers of particles were delivered per unit area using the concentration in the 24-well plate initial study as reference. We tried as much as possible to stick to 24-well plates in this study.

Mn nanoparticle characterization and uptake

N27 dopaminergic neurons (~300,000) were grown on poly-L or poly-D lysine coated cover slips in six-well plates. They were then treated with 50 μg/ml of nanoparticles suspended in culture growth medium for up to 6 h. Both untreated controls and treated cells were used for live cell imaging of the uptake using DIC microscopy, as previously described (Sun *et al*., 2008), or fixed and processed for TEM microscopy (Hussain *et al*., 2006).

N27 dopaminergic neuronal cells were grown on coverslips (~ 2.5×10^5) in six-well plates, treated with Mn nanoparticles at the appropriate time points, and then fixed with 2% glutaraldehyde (w/v) and 2% paraformaldehyde (w/v) in 0.1 M sodium cacodylate buffer, pH 7.2, for 24 h at 4°C. The samples were washed in buffer and subsequently fixed in 1% osmium tetroxide in 0.1 M cacodylate buffer for 1 h (room temperature). Following the fixation, the samples were dehydrated with 70% ethanol, contrast stained with 2% uranyl acetate in 75% ethanol for 30 min, and further dehydrated in a graded ethanol series. They were then cleared with ultra-pure acetone, infiltrated and embedded using a modified EPON epoxy resin (Embed 812; Electron Microscopy Sciences, Ft. Washington, PA). Resin blocks were polymerized for 48 h at 70°C. Thick and ultrathin sections were made using a Leica UC6 ultramicrotome (Leeds Precision Instruments, Minneapolis, MN). Ultrathin sections were collected onto copper grids and images were captured using a JEM 2100 200kV scanning and transmission electron microscope (Japan Electron Optic Laboratories, USA, Peabody, MA).

Assessment of cell death by Sytox Green assay

Cytotoxicity assessment was carried out using Sytox Green, a membrane-impermeable DNA dye that enters dead cells with compromised cell membranes as a result of altered membrane permeability, intercalating the nucleic acid, as described previously (Song *et al*., 2010). An excitation wavelength of 485 nm and an emission wavelength of 538 nm can be used to detect the DNA-bound Sytox Green using a fluorescence microplate reader (BioTek microplate reader, BioTek Instruments, Winooski, Vermont, USA). The fluorescence intensity is directly proportional to the number of dead cells. This method has been reported to be more efficient and sensitive than other cytotoxicity measurements (Kitazawa *et al*., 2004). The same numbers of subconfluent N27 cells were grown in 24-well plates for 16–18 h, co-incubated with either 1 μM Sytox Green and appropriate Mn nanoparticle concentrations or RPMI culture medium as a control. Fluorescence intensity was monitored at appropriate time points during the experiments to quantify the resulting cell death, and fluorescence pictures were taken using a Nikon inverted fluorescence microscope equipped with a SPOT digital camera (Diagnostic Instruments, Sterling Heights, MI).

Determination of mitochondrial superoxide production by MitoSOX

N27 dopaminergic cells (~ 250,000 per well) were grown in glass bottom dishes 16–18 h prior to treatments and then exposed to 50 μg/mL Mn nanoparticles for up to 4.5 h. Mitochondrial superoxide production in the cells was measured using MitoSOX fluorescence probe in Hank's Buffered Salt Solution (HBSS) containing calcium and magnesium, according to the manufacturer's protocol. MitoSOX was added to a final concentration of 5 μM in HBSS. Cells were allowed to load MitoSOX for 30 min and the cells were washed twice with HBSS (Mukhopadhyay *et al*., 2007). A Nikon inverted fluorescence microscope equipped with a SPOT digital camera (Diagnostic Instruments, Sterling Heights, MI) was used for taking fluorescent pictures. The cells were kept in a CO_2 incubator at 37°C in between observations.

Determination of Mn nanoparticle-induced H_2O_2 production by 5-(and-6)-chloromethyl-2′, 7′-dichlorodihydrofluorescein diacetate (CM-H_2DCFDA, Molecular Probes)

The production of ROS has been widely measured using a fluorescent probe, 5- (and-6)-chloromethyl-2′,7′-dichlorodihydrofluorescein diacetate (CM-H_2DCFDA, Molecular Probes) (Gao *et al*., 2003; Mao *et al*., 2007). We measured ROS generation in Mn nanoparticle treated N27 cells, as described in our recent publication, with a slight modification (REF). N27 cells (~ 10,000 per well) were grown in 96-well plates 16–18 h prior to treatments and then exposed to Mn nanoparticles. H_2O_2 production in the cells was measured using CM-H_2DCFDA following exposure to 50 μg/mL Mn nanoparticles for up to 3 h. CM-H_2DCFDA was added to a final concentration of 10 μM in phenol red -free Hank's Buffered Salt Solution (HBSS) containing calcium and magnesium, according to the manufacturer's recommendation. Cells were allowed to load CM-H_2DCFDA for 15–20 min and the cells were washed with HBSS. The fluorescence was measured using a Synergy HT microplate reader (BioTek Instruments, Winooski, Vermont, USA), fluorescence (excitation 488nm, emission 515 nm).

Western blotting

N27 dopaminergic neuronal cells were exposed to 50 μg/mL Mn nanoparticles with or without either the pan-caspase inhibitor (Z-VAD-FMK) and/or caspase-3 inhibitor (Z-DEVD-FMK) at 37°C for appropriate experimental time points. Following exposure, the N27 cells were lysed, homogenized, sonicated, and centrifuged, as described previously (Kaul *et al*., 2003b; Kitazawa *et al*., 2003; Afeseh Ngwa *et al*., 2009). Cells were lysed using the modified RIPA buffer. The supernatants were collected as cell lysates, and protein concentrations were normalized, after determining protein concentrations by the Bradford assay, and used for SDS-gel electrophoresis. Whole cell lysates with equal protein amounts were loaded in each lane and separated on a 10–15% SDS-PAGE gel, depending on the protein size, as described previously (Kaul *et al*., 2003b; Kitazawa *et al*., 2003). The proteins on the gels were then transferred to nitrocellulose membranes, and non-specific binding sites were blocked by incubation in Licor buffer for 1 h. Following blocking, the membranes were then incubated in the appropriate primary antibodies, PKCδ polyclonal antibody (1:1000), Beclin 1 (1:500), caspase-3 (1:500), LC3(1:2000), Tf (1:1000), washed and subsequently incubated with appropriate secondary anti-mouse or anti-rabbit antibodies. To confirm equal protein loading in each lane, membranes were reprobed with β-actin antibody (1:5000 dilution). Western blotting was performed using IR dye-800 conjugated anti-rabbit dye and Alexa Fluor 680 conjugated anti-mouse IgG as secondary antibodies. The blot images were captured and analyzed using an Odyssey IR Imaging system (LICOR from Licor Biosciences).

Determination of autophagy by GFP-LC3 expression

GFP-LC3 has been observed through fluorescence microscopy either as a diffuse cytoplasmic pool in control cells or as punctate structures representative of the levels of autophagy in the cells, as described recently (Mizushima and Yoshimori, 2007; Tanida *et al*., 2008; Mizushima *et al*., 2010). N27 dopaminergic cells were transiently transfected with either GFP-LC3 (wild type) or GFP-LC3-ΔG (mutant). The cells were resuspended in transfection buffer to a final concentration of 5 million neurons/100 μl and mixed with 5 μg of the plasmid DNA. Electroporation was performed using an Amaxa Nucleofector instrument, according to the manufacturer's protocol. The transfected N27 cells were then plated at a density of 2.5×10^5 in glass bottom dishes for 24 h and then treated with 50 μg/mL Mn nanoparticles for different time points. Fluorescent microphotographs of GFP-LC3 were taken at these time points with a SPOT digital camera and analyzed with MetaMorph software (Universal Imaging Corporation, Downingtown, PA, USA).

Immunocytochemistry

Following exposure to the appropriate concentration of Mn nanoparticles, the primary mesencephalic neurons were fixed with 4% paraformaldehyde and processed for immunocytochemical staining. First, nonspecific sites were blocked with buffer comprising 2% bovine serum albumin (BSA), 0.05% Tween-20 and 0.5% Triton X-100 in phosphate-buffered saline (PBS) for 1 h. Cells were subsequently washed thrice with PBS and incubated with antibody directed against TH (1:1500 dilution) at 4°C overnight. The cells were again washed with PBS, followed by incubation with Cy3-conjugated (red; 1:1000) secondary antibody for 90 min at room temperature. Incubation with 10 μg/ml Hoechst 33342 nuclear stain for 5 min at room temperature followed incubation with secondary antibody. Each batch of embryos was processed under identical conditions. The stained cells on the coverslips were washed with PBS, mounted on a slide, and viewed under a Nikon inverted fluorescence microscope (model TE-2000U; Nikon, Tokyo, Japan). The images were captured with a SPOT digital camera (Diagnostic Instruments, Inc., Sterling Heights, MI).

Quantification of TH^+ cell count and neuronal processes

The number of TH^+ cells was counted from at least eight different fields on each coverslip from both the controls and the treatment groups. We first identified a threshold for the images, before the neuronal counts were made using the Integrated Morphometry Analysis (IMA) function in the Metamorph image analysis software (Molecular Devices, Downingtown, PA). The MetaMorph software, version 5.0 (Molecular Devices, Sunnyvale, CA), was used to measure the neurite length of the primary neurons of the TH^+ cells from each coverslip in the control and treatment groups. The data were pooled from at least eight different fields from each of the 8 cover slips per treatment group. The lengths of the processes were marked by applying the region and length measurement function in the IMA. The data were logged to an Excel spreadsheet (Microsoft, Redmond, WA), then exported and analyzed using Graph Pad Prism 5.0 software. TH^+ neurons were counted and their processes were measured in at least eight individual cultures for each treatment. This is a slightly modified method from a method recently used for quantification of neuronal processes (Yang *et al*., 2004; Sun *et al*., 2006).

Statistical analysis

Data were analyzed using Prism 5.0 software (GraphPad Software, San Diego, CA). In order to compare differences between more than two treatment groups we used Tukey's multiple comparison testing. For comparison between two samples, the Student's T-test was performed to examine the differences. Differences with * $p<0.05$, ** $p<0.01$, and

***p<0.001 were considered significant and are indicated by asterisks. Presented data typically represent results from at least two separate experiments with at least triplicate samples where appropriate, and are expressed as mean ± S.E.M.

Results

Characterization of Mn nanoparticles using TEM and DIC microscopy

We first characterized the size of the Mn nanoparticles both singly and in agglomerates before we used them for experiments. Mn nanoparticles were mixed with cell culture media at a concentration of 20 mg/mL, the stock concentration from which the working concentrations are derived. The mean sizes of the nanoparticles were calculated using TEM software, as described in the methods. We also used a new DIC method to estimate the nanoparticle sizes, as described in our recent publication (Sun *et al*., 2008). As depicted in Fig.1, we observed that the nanoparticles ranged in size from single nanoparticles as small as ~ 20 nm (Fig. 1A) to agglomerates 100~ 900 nm in size (Fig. 1B). These results show that our Mn nanoparticle solution prepared for the cell culture experiments contained a mixture of nanosize materials as well as agglomerates.

Uptake of Mn nanoparticles in N27 dopaminergic neuronal cells

Following the characterization of nanosized Mn particles in solution, we examined whether Mn nanoparticles are actually taken up by N27 dopaminergic neuronal cells. Since characterization of *in vitro* nanoparticle uptake and localization is directly linked to cytotoxicity, uptake studies provide further evidence of nanoparticle-cell interaction with intracellular machinery. Dopaminergic N27 cells were grown on polylysine-coated cover slips, as described in the methods. They were then treated with 50 μg/mL nanoparticles suspended in culture growth medium for up to 6 h. Both untreated controls and treated cells were fixed and processed for TEM microscopy (Fig. 2A and 2B) or used for live cell imaging of the uptake using DIC microscopy (Fig. 2C and 2D). Using both microscopy methods, we showed that the nanoparticles enter the cells. The results further revealed that the particles are engulfed in the membrane and then translocate to cytosol.

Mn nanoparticles upregulate Transferrin (Tf) levels in N27 dopaminergic cells

To determine whether the Mn nanoparticles that enter the cells evoke a biological response, we measured the level of transferrin (Tf) in cells exposed to Mn nanomaterials. Tf is a major metal transport protein in CNS that binds several metals including Mn, mediating their transport (Aschner and Aschner, 1991). We observed a time-dependent increase in the levels of Tf at the 3, 6, and 9 h time points following exposure to 50 μg/mL Mn nanoparticles, as measured by Western blotting (Fig. 3). These results suggest that internalized Mn nanoparticles can cause upregulation of the major metal transporter protein.

Mn nanoparticle exposure induces dose- and time-dependent increase in cytotoxicity in N27 dopaminergic cells

In order to determine the optimal dose for a mechanistic investigation of Mn nanoparticle neurotoxicity, we first performed a dose-response and time-dependent cytotoxicity analysis. N27 dopaminergic cells were exposed to 25–400 μg/mL of Mn nanoparticles in 24-well plates for 6 h, and a dose-dependent effect of Mn nanoparticles on cytotoxic cell death was determined by Sytox assay. The Sytox Green dye labels only dead or dying cells and the resulting green fluorescence can be measured both qualitatively and quantitatively. Mn nanoparticles increased cell death in a dose-dependent manner and the quantitative dose-dependent decrease in cell viability was observed by quantifying the Sytox fluorescence. As

shown in Fig. 4A, exposure to 25, 50, 100, 200 and 400 μg/mL of Mn nanoparticles over 6 h resulted in a good dose response of cytotoxicity as compared to control cells.

A time-dependent effect of Mn nanoparticle-induced cell death was also observed using the Sytox Green fluorescence assay. N27 cells were exposed to 50 μg/mL of Mn nanoparticles for 3, 6, and 9 h. Fig. 4B quantitatively shows significant increases in cell death over time. The cell death began at 3 h of Mn nanoparticle exposure and the maximal cell death was observed at the 9 h time point (Fig. 4B). Visualization of Sytox positive cells under fluorescence microscope further confirmed increased cell death following Mn nanoparticle exposure in dopaminergic neuronal cells compared to untreated controls (Fig. 4C).

Mn nanoparticle exposure induces oxidative stress in dopaminergic neuronal N27 cells

Based on the cytotoxicity data, we chose an optimal dose of 50 μg/mL nanoparticles for most of the subsequent experiments. Several other studies, including those from our lab, have shown that dopaminergic neurotoxicants, including MPP^+, Mn in its organic and inorganic forms, vanadium, and dieldrin, induce oxidative stress, modulate mitochondrial function and mediate the release of a number of proapoptotic factors (Kitazawa *et al*., 2001b; Anantharam *et al*., 2002; Kaul *et al*., 2003b; Kanthasamy *et al*., 2005) to initiate the apoptotic cell signaling cascade. We therefore examined whether Mn nanoparticle exposure induces ROS production in dopaminergic cells. We probed both the cytoplasmic and mitochondrial ROS generation. The production of cytoplasmic peroxide was measured using a fluorescent probe, 5- (and-6)-chloromethyl-2′,7′-dichlorodihydrofluorescein diacetate (CM-H_2DCFDA, Molecular Probes), as described in the methods. We observed that there was approximately a two-fold increase in ROS at the 2 h time point and about a six-fold increase at the 3 h time point (Fig. 5A). We also qualitatively measured the induction of mitochondrial superoxide by Mn nanoparticles using MitoSOX. We observed increased superoxide production in the mitochondria of the Mn nanoparticle treated cells, as shown by the increased red intensity in the pictures, compared to the untreated control (Fig. 5B). These results collectively suggest that Mn nanoparticle exposure induces oxidative stress in dopaminergic neuronal cells possibly by impairing mitochondrial function.

Mn nanoparticles induce an increase in caspase-3 and PKCδ activity

We have demonstrated in our laboratory that a number of neurotoxicants, including metals, can promote an oxidative stress mediated apoptotic cell signaling cascade in dopaminergic neuronal cells via the novel PKC isoform, PKCδ (Kanthasamy, 2003; Kanthasamy *et al*., 2003a; Kanthasamy *et al*., 2003b; Latchoumycandane *et al*., 2005; Afeseh Ngwa *et al*., 2009). Caspase-3 cleaves PKCδ to yield a 41 kDa catalytically active subunit and a 38 kDa regulatory subunit, resulting in a sustained activation of the kinase. Notably, we demonstrated that inorganic Mn induced the proteolytic cleavage of PKCδ, but not of PKCα, β, or γ in an isoform specific and caspase-3 dependent manner (Latchoumycandane *et al*., 2005). In the present study, we therefore examined whether Mn nanoparticles induce caspase-3 dependent proteolytic activation of PKCδ. First, we observed that Mn nanoparticle exposure results in an increase in caspase-3 activation, as shown by increased caspase-3 cleavage by Western blot (Fig. 6). The caspase-3 activation was found to be time-dependent. Importantly, co-treatment with 100 μM of the caspase inhibitor Z-VAD-FMK reduced Mn nanoparticle-induced caspase-3 activation to a level nearly equal to untreated control levels, demonstrating the specificity of caspase activation during Mn nanoparticle exposure (Fig. 6A).

The increase in caspase-3 activation subsequently proteolytically cleaved PKCδ in Mn nanoparticle-treated N27 dopaminergic neuronal cells in a time-dependent manner at the 3, 6, and 9 h time points (Fig. 7A). Additionally, we used the pharmacological and cell-

permeable caspase inhibitors to confirm that PKCδ cleavage is mediated by a caspase-dependent mechanism. Co-treatment with either 100 μM of the pan-caspase inhibitor Z-VAD-FMK or 50 μM of the caspase-3 specific inhibitor Z-DEVD-FMK moderately reduced Mn nanoparticle-induced PKCδ cleavage (Fig. 7B), suggesting that the cleavage is indeed mediated by caspase-3. In addition, our experiments also revealed a time-dependent increase in the phosphorylation of PKCδ activation loop at the Threonine 505 site following exposure to 50 μg/mL Mn nanoparticles, indicative of PKCδ activation (Fig. 7C). The nitrocellulose membranes were reprobed with the β-actin antibody to confirm equal protein loading.

Mn nanoparticles induce cell death independent of oxidative stress

To further explore the role of oxidative stress in Mn nanoparticle-induced dopaminergic neuronal cell death, we tested the effect of antioxidants on cell death. We carried out experiments using 2% B27 with an antioxidant cocktail (AO) consisting of vitamin E, glutathione, superoxide dismutase (SOD), and catalase, as described in the methods. This cocktail has been shown to produce a strong antioxidant effect against oxidative damage (Toh *et al*., 2008; Afeseh Ngwa *et al*., 2009). N27 cells were exposed to 50 μg/mL Mn nanoparticles co-treated with or without AO for 9 h, and then cytotoxicity was measured by Sytox Green fluorescence assay. Co-treatment with AO failed to reduce or block the neurotoxicity produced by Mn nanoparticles (Fig. 8), suggesting that Mn nanoparticles-induced oxidative stress does not play a causal role in the nanoparticle toxicity.

Mn nanoparticles induce autophagy in dopaminergic neuronal cells

Given the recent attention that autophagy has received as an alternative cell death pathway in neurodegenerative diseases, especially PD (Cheung and Ip, 2009), we proceeded to measure whether autophagy might also play a role in the observed Mn nanoparticle-induced cell death. Recently, we showed an increase in autophagy in N27 dopaminergic neuronal cells following neurotoxic insult (Kanthasamy *et al*., 2006). Beclin 1 has also been found to be a key marker of autophagy. In a recent study, Wirawan *et al*. (2010) reported that cleavage of Beclin 1 may be a critical factor in modulating the cells from a protective autophagic pathway into apoptotis. In this study, we observed a significant increase in Beclin 1 cleavage over the 3, 6, and 9 h time points in N27 dopaminergic cells following exposure to 50 μg/mL Mn nanoparticles (Fig. 9A).

LC 3 has been shown to be a key marker of autophagy induction. The level of cytoplasmic LC3 (LC3 I) is gradually processed and recruited to LC3 II in the autophagosomes. LC3 Western blotting usually reveals an LC3-I (18 kDa) and LC3-II (16 kDa), with the degree of increased levels of LC3-II correlating well with increase in autophagy (Tanida *et al*., 2008). We observed an increase in LCII levels with a concomitant decrease in LCI levels over the 3, 6, and 9 h time points in N27 cells following exposure to 50 μg/mL Mn nanoparticles (Fig. 9B). We further confirmed the induction of autophagy by visualizing GFP-LC3 accumulation in N27 dopaminergic cells transfected with either GFP-LC3 or GFP-LC3-ΔG. As shown in Fig. 9 C, an increased accumulation of LCII puncta following exposure to the nanoparticles, as opposed to a more diffuse and less pronounced green staining in the control cells, was observed, indicative of an autophagic phenotype.

Mn nanoparticles induce neurotoxic responses to primary dopaminergic neurons

To further demonstrate that Mn nanoparticles are toxic to nigral dopaminergic neurons, we exposed mouse primary mesencephalic neuronal cultures to 25 and 50 μg/mL Mn nanoparticles for 24 h. Following exposure, we then assessed the viability of dopaminergic neurons by counting the number of dopaminergic neurons and measuring their neurite lengths. We observed a significantly reduced number of dopaminergic neurons (Fig. 10A and 10C) and neurite lengths (Fig. 10B and 10C) in Mn nanoparticle treated cells relative to

control cultures. This further indicates that manganese nanoparticles can induce a neurotoxic effect in nigral dopaminergic neurons.

Discussion

We demonstrate for the very first time that Mn nanoparticles can enter mesencephalic dopamine-producing neuronal cells, where they induce oxidative stress and cell death through the activation of a previously established apoptotic cascade involving caspase-3 activation and the proteolytic cleavage of PKCδ. Our results further suggest the induction of autophagy by Mn nanoparticles. We used the pharmacological inhibitors, pan-caspase inhibitor Z-VAD-FMK and caspase-3 specific inhibitor Z-DEVD-FMK, to confirm that the caspase-mediated, PKCδ signaling proapoptotic cascade plays a role during Mn nanoparticle-induced apoptosis in dopaminergic neuronal cells. Our results also indicate that Mn nanoparticles upregulate the metal transporter protein Transferrin in dopaminergic neuronal cells, but the cell death appears to be mediated independent of oxidative stress. Our observations from experiments with primary mesencephalic cultures following Mn nanoparticle exposure further confirm that Mn nanoparticles can induce degeneration of nigral dopaminergic neurons.

Nanoparticles are useful in many areas of science and technology, but improper use and handling of nanomaterials might have adverse effects on human health due to their combined effect of small size and reactive properties. Their small size and consequential large surface area may allow them ready access and entry into cells and tissues. Nanoparticles may enter via various routes, including inhalation, ingestion, and absorption by skin. Once these nanoparticles enter the body, they can translocate to sites far away from their site of entry because of their minute size (Oberdorster *et al*., 2005). Translocation of nanoparticles first occurs across cell membranes and then transfer to other cells and even to entire organ. In nervous tissue, nanomaterials can move along the axons and dendrites that connect adjacent neurons and non-neuronal cells. After instillation or inhalation, nanoparticles can indeed enter the brain via the *nervus olfactorius*, following deposition on the olfactory mucosa of the nose (Oberdorster *et al*., 1995). This increases the potential for nanoparticle entry into the central nervous system, especially the brain, causing toxicity to sensitive neurons like dopaminergic neurons. A previous study reported that 40 nm Mn nanoparticles and agglomerates were effectively internalized by adrenal tumor cells commonly known as PC-12 cells, increasing oxidative stress and depleting dopamine levels and its metabolites (Hussain *et al*., 2006). The doses were similar to those used in this study, demonstrating that the 50 μg/mL dose is neurotoxic (Hussain *et al*., 2006). In our study, we demonstrate that Mn nanoparticles exposures at doses up to 50 μg/ml resulted in internalization of particles as small as 20 nm in dopaminergic neuronal cells.

Transferrin (Tf) is one of the major metal transport proteins in the CNS, and it has been reported to bind several metals including Fe, Mn, Zn, and Cr as well as Cu, Co, Cd, V and Al, mediating their transport in the brain (Aschner and Aschner, 1991). Similarly, Erikson *et al*. have also shown that Mn and Fe can be transported in a Tf-dependent manner (Erikson *et al*., 2004). In this study, we observed a time-dependent increase in the protein levels of Tf, suggesting that Tf may play a role in the uptake of Mn nanoparticles by dopaminergic neurons. Our results also suggest that Mn nanoparticle exposure may sensitize the cells to metal toxicity by increasing uptake of metals via Transferrin upregulation. It is also possible that transferrin receptors could be upregulated by Mn-dependent ROS ensuing from free metal liberated by endosomal/lysosomal systems. Therefore, further studies are needed to clarify the exact mechanisms of Mn nanoparticle transport in the dopaminergic system in relation to the metal transport proteins.

We have already shown in our laboratory that exposure to organic and inorganic forms of Mn leads to the generation of ROS, with accompanying depolarization of the mitochondrial membrane potential in dopaminergic neuronal cells (Anantharam *et al*., 2002; Kitazawa *et al*., 2002). Kitazawa *et al*. (2002) observed that dopaminergic neuronal cells showed a greater vulnerability to Mn-induced ROS generation and apoptotic cell death than non-dopaminergic cells (Kitazawa *et al*., 2002), suggesting that dopaminergic neurons have an increased sensitivity to metal neurotoxic insult. Based on previous studies, one of the reasons for this increased susceptibility of dopaminergic neurons to metal-induced neurotoxicity is that metals in a ROS-rich environment tend to augment oxidative insult through the formation of dopamine-derived highly cytotoxic radicals (Junn and Mouradian, 2001; Kitazawa *et al*., 2001a; Kanthasamy, 2002). It has been reported that Mn ions can oxidize monoamines like serotonin and dopamine (Segura-Aguilar and Lind, 1989; Lloyd, 1995). Increases in the generation of ROS offset homeostasis of the mitochondrial environment, which is critical for oxidative phosphorylation and initiation of peroxidative decomposition of phospholipids, hence compromising the integrity of cellular membranes and leading to the propagation of cellular injury (Kokoszka *et al*., 2001). We observed in the current study that exposure to Mn nanoparticles increased the generation of both cytoplasmic peroxide and mitochondrial superoxide in dopaminergic cells.

We previously reported that antioxidants can attenuate apoptotic cell death induced by neurotoxic chemicals, including heavy metals, by blocking the generation of ROS (Kitazawa *et al*., 2002; Kaul *et al*., 2003b; Afeseh Ngwa *et al*., 2009). However, in the present study, Mn nanoparticle co-treatments with an antioxidant cocktail consisting of vitamin E, catalase, superoxide dismutase (SOD) and glutathione failed to protect the cells from Mn nanoparticle-induced neurotoxicity. Although ROS is critical for apoptotic cell death, other studies have found that blocking ROS failed to rescue the cells from death (Gunasekar *et al*., 2001; Chen *et al*., 2008). Together, our results suggest that while oxidative stress might play a role in the initiation of the neurotoxic signaling cascade during Mn nanoparticle exposure, the oxidative stress independent pathways might contribute to execution of the neurotoxicity.

It has been established that the caspases, especially effector caspase-3, have an important function in the execution of apoptosis in dopaminergic neuronal cells (Cassarino and Bennett, 1999; Dodel *et al*., 1999; Anantharam *et al*., 2002; Kanthasamy *et al*., 2003a; Kaul *et al*., 2003a). We observed that Mn nanoparticle exposure increased caspase-3 cleavage over time. This critical role of caspase-3 activation as a key player in the apoptotic cascade in dying dopaminergic neurons has also been demonstrated in human PD patients as well as in animal models of the disease (Hartmann *et al*., 2000). We have demonstrated that the proteolytic activation of PKCδ by caspase-3 is an important event in the apoptotic cell death of dopaminergic cells after neurotoxic insults (Kanthasamy *et al*., 2003a; Kaul *et al*., 2005). In previous studies, we showed that the organic form of Mn, MMT (Methylcyclopentadienyl manganese tricarbonyl), or inorganic Mn can induce caspase-3-dependent proteolytic cleavage of PKCδ following exposure in an isoform-specific manner (Anantharam *et al*., 2002; Latchoumycandane *et al*., 2005). Importantly, the proteolytic activation of PKCδ contributes to Mn-induced cell death (Anantharam *et al*., 2002; Latchoumycandane et al., 2005). In this study, we showed that exposure to Mn nanoparticles resulted in a time-dependent PKCδ proteolytic cleavage. Co-treatment with the pan-caspase inhibitor Z-VAD-FMK and caspase-3-specific inhibitor Z-DEVD-FMK moderately blocked Mn nanoparticle-induced PKCδ proteolytic cleavage, suggesting that PKCδ activation is caspase-3 dependent during Mn nanoparticle exposure in N27 dopaminergic neuronal cells. In addition to proteolytic activation, PKCδ phosphorylation at Thr-505 was also observed during Mn nanoparticle exposure, suggesting the additional activation of the kinase. Oxidative insult by H_2O_2 has been shown to enhance phosphorylation of PKCδ at Thr-505, resulting in

increased PKCδ enzymatic activity (Konishi *et al*., 1997). Collectively, we demonstrate for the first time Mn nanoparticle exposure can activate a key proapoptotic kinase in dopaminergic neuronal cells. The signaling events, which are downstream of PKCδ activation and finalize the apoptotic cell death cascade, are yet to be clarified.

Autophagy has gained considerable interest in recent years for its role in neurodegenerative disorders because autophagy serves as a complimentary cell death pathway to apoptosis (Anglade *et al*., 1997; Oztap and Topal, 2003). We sought to carry out some experiments to determine if Mn nanoparticle exposure might also activate an alternative autophagic cell death pathway in dopaminergic neurons. We observed a decrease in the native form of Beclin1 and an increase in cleavage, together with increases in LC3II, which are typically associated with the formation of autophagosomes. Recently, gold nanoparticles were shown to cause autophagy (Li *et al*., 2010). Different types of stressors can up-regulate LC3 and promote the conjugation of its cytosolic form, LC3 I, to phosphatidylethanolamine, constituting the autophagosome-specific LC3 II, which serves as the most reliable marker of autophagy (Kabeya *et al*., 2000; Klionsky *et al*., 2008). In addition to LC3 II, Beclin-1 is recognized as an important regulator of autophagy (Pattingre *et al*., 2005; Wirawan *et al*., 2010). The binding of Beclin-1 to Bcl-2 or Bcl-x_L inhibits the autophagic function of Beclin-1 (Pattingre *et al*., 2005; Maiuri *et al*., 2007a; Maiuri *et al*., 2007b), suggesting that Beclin-1 might play a role in the convergence between autophagy and apoptotic cell death. Wirawan *et al*. (2010) demonstrated the interplay between autophagy and apoptosis mediated by caspase-mediated cleavage of Beclin-1 into a smaller Beclin-1-C fragment, which further enhanced the apoptotic pathway (Wirawan *et al*., 2010). Together, our results suggest that autophagy might also play a role in Mn nanoparticle-induced cell death.

As summarized in Fig. 11, we demonstrate that Mn nanoparticle exposure can in fact be neurotoxic to dopaminergic neurons by activating more than one cell death pathway involving both apoptosis and autophagy. Our results further demonstrate that Mn nanoparticles induce oxidative stress, but the oxidative stress does not seem to be a major mediator of the neurotoxicity. Further investigation of the possible interaction of autophagy and apoptosis in nigral dopaminergic neurons using both cell culture and animal models of Mn nanoparticle toxicity will provide greater mechanistic insights into nano-neurotoxicology. Future studies in animal models should enhance understanding of the health effects of manganese nanoparticles and may guide the risk assessment of metal nanoparticles by regulatory agencies.

Research Highlights

- Mn nanoparticles effectively enter dopaminergic neuronal cells and activate the mitochondrial-apoptotic signaling pathway.
- Mn nanoparticles activate caspase-mediated proteolytic cleavage of a proapoptotic PKCδ cascade.
- Mn nanoparticles induce autophagy in dopaminergic neuronal cells
- Exposure to Mn nanoparticles to primary mesencephalic neurons induces loss of TH+ dopaminergic neurons.
- The study emphasizes potential neurotoxic health risks of Mn nanoparticles to the nigral dopaminergic system.

Acknowledgments

We are grateful to QuantumSphere, Inc. (Santa Ana, CA) for supplying the nanoparticles used in this study. This work was supported by National Institutes of Health (NIH) Grants ES10586 and ES19267. The W. Eugene and Linda Lloyd Endowed Chair to AGK is also acknowledged. The authors acknowledge Mrs. MaryAnn Devries for her assistance in the preparation of this manuscript.

References

Afeseh Ngwa H, Kanthasamy A, Anantharam V, Song C, Witte T, Houk R, Kanthasamy AG. Vanadium induces dopaminergic neurotoxicity via protein kinase Cdelta dependent oxidative signaling mechanisms: relevance to etiopathogenesis of Parkinson's disease. Toxicol Appl Pharmacol. 2009; 240:273–285. [PubMed: 19646462]

Anantharam V, Kitazawa M, Wagner J, Kaul S, Kanthasamy AG. Caspase-3-dependent proteolytic cleavage of protein kinase Cdelta is essential for oxidative stress-mediated dopaminergic cell death after exposure to methylcyclopentadienyl manganese tricarbonyl. J Neurosci. 2002; 22:1738–1751. [PubMed: 11880503]

Anglade P, Vyas S, Javoy-Agid F, Herrero MT, Michel PP, Marquez J, Mouatt-Prigent A, Ruberg M, Hirsch EC, Agid Y. Apoptosis and autophagy in nigral neurons of patients with Parkinson's disease. Histol Histopathol. 1997; 12:25–31. [PubMed: 9046040]

Aschner M, Aschner JL. Manganese neurotoxicity: cellular effects and blood-brain barrier transport. Neurosci Biobehav Rev. 1991; 15:333–340. [PubMed: 1956602]

Aschner M, Erikson KM, Dorman DC. Manganese dosimetry: species differences and implications for neurotoxicity. Crit Rev Toxicol. 2005; 35:1–32. [PubMed: 15742901]

Aschner M, Lukey B, Tremblay A. The Manganese Health Research Program (MHRP): status report and future research needs and directions. Neurotoxicology. 2006; 27:733–736. [PubMed: 16325914]

Balshaw DM, Philbert M, Suk WA. Research strategies for safety evaluation of nanomaterials, Part III: nanoscale technologies for assessing risk and improving public health. Toxicol Sci. 2005; 88:298–306. [PubMed: 16162851]

Borm P, Klaessig FC, Landry TD, Moudgil B, Pauluhn J, Thomas K, Trottier R, Wood S. Research strategies for safety evaluation of nanomaterials, part V: role of dissolution in biological fate and effects of nanoscale particles. Toxicol Sci. 2006; 90:23–32. [PubMed: 16396841]

Braydich-Stolle L, Hussain S, Schlager JJ, Hofmann MC. In vitro cytotoxicity of nanoparticles in mammalian germline stem cells. Toxicol Sci. 2005; 88:412–419. [PubMed: 16014736]

Cassarino DS, Bennett JP Jr. An evaluation of the role of mitochondria in neurodegenerative diseases: mitochondrial mutations and oxidative pathology, protective nuclear responses, and cell death in neurodegeneration. Brain Res Brain Res Rev. 1999; 29:1–25. [PubMed: 9974149]

Chen Y, McMillan-Ward E, Kong J, Israels SJ, Gibson SB. Oxidative stress induces autophagic cell death independent of apoptosis in transformed and cancer cells. Cell Death Differ. 2008; 15:171–182. [PubMed: 17917680]

Cheung ZH, Ip NY. The emerging role of autophagy in Parkinson's disease. Mol Brain. 2009; 2:29. [PubMed: 19754977]

Clarkson ED, Edwards-Prasad J, Freed CR, Prasad KN. Immortalized dopamine neurons: A model to study neurotoxicity and neuroprotection. Proc Soc Exp Biol Med. 1999; 222:157–163. [PubMed: 10564540]

Cui D, Gao H. Advance and prospect of bionanomaterials. Biotechnol Prog. 2003; 19:683–692. [PubMed: 12790626]

Dodel RC, Du Y, Bales KR, Ling Z, Carvey PM, Paul SM. Caspase-3-like proteases and 6-hydroxydopamine induced neuronal cell death. Brain Res Mol Brain Res. 1999; 64:141–148. [PubMed: 9889353]

Erikson KM, Syversen T, Steinnes E, Aschner M. Globus pallidus: a target brain region for divalent metal accumulation associated with dietary iron deficiency. J Nutr Biochem. 2004; 15:335–341. [PubMed: 15157939]

Gao HM, Liu B, Zhang W, Hong JS. Novel anti-inflammatory therapy for Parkinson's disease. Trends Pharmacol Sci. 2003; 24:395–401. [PubMed: 12915048]

Guilarte TR. Manganese and Parkinson's Disease: A Critical Review and New Findings. Environ Health Perspect. 2010; 118

Gunasekar P, Li L, Prabhakaran K, Eybl V, Borowitz JL, Isom GE. Mechanisms of the apoptotic and necrotic actions of trimethyltin in cerebellar granule cells. Toxicol Sci. 2001; 64:83–89. [PubMed: 11606804]

HaMai D, Bondy SC. Oxidative basis of manganese neurotoxicity. Ann N Y Acad Sci. 2004; 1012:129–141. [PubMed: 15105260]

Han MJ, Ozaki T, Yu J. Electronic structure and magnetic properties of small manganese oxide clusters. J Chem Phys. 2005; 123:34306. [PubMed: 16080736]

Hartmann A, Hunot S, Michel PP, Muriel MP, Vyas S, Faucheux BA, Mouatt-Prigent A, Turmel H, Srinivasan A, Ruberg M, Evan GI, Agid Y, Hirsch EC. Caspase-3: A vulnerability factor and final effector in apoptotic death of dopaminergic neurons in Parkinson's disease. Proc Natl Acad Sci U S A. 2000; 97:2875–2880. [PubMed: 10688892]

Holsapple MP, Farland WH, Landry TD, Monteiro-Riviere NA, Carter JM, Walker NJ, Thomas KV. Research strategies for safety evaluation of nanomaterials, part II: toxicological and safety evaluation of nanomaterials, current challenges and data needs. Toxicol Sci. 2005; 88:12–17. [PubMed: 16120754]

Hussain SM, Hess KL, Gearhart JM, Geiss KT, Schlager JJ. In vitro toxicity of nanoparticles in BRL 3A rat liver cells. Toxicology in Vitro. 2005; 19:975–983. [PubMed: 16125895]

Hussain SM, Javorina AK, Schrand AM, Duhart HM, Ali SF, Schlager JJ. The interaction of manganese nanoparticles with PC-12 cells induces dopamine depletion. Toxicol Sci. 2006; 92:456–463. [PubMed: 16714391]

Jayakumar AR, Rama Rao KV, Kalaiselvi P, Norenberg MD. Combined effects of ammonia and manganese on astrocytes in culture. Neurochem Res. 2004; 29:2051–2056. [PubMed: 15662839]

Junn E, Mouradian MM. Apoptotic signaling in dopamine-induced cell death: the role of oxidative stress, p38 mitogen-activated protein kinase, cytochrome c and caspases. J Neurochem. 2001; 78:374–383. [PubMed: 11461973]

Kabeya Y, Mizushima N, Ueno T, Yamamoto A, Kirisako T, Noda T, Kominami E, Ohsumi Y, Yoshimori T. LC3, a mammalian homologue of yeast Apg8p, is localized in autophagosome membranes after processing. Embo J. 2000; 19:5720–5728. [PubMed: 11060023]

Kanthasamy A. A novel proteolytic activation of PKC delta promotes apoptotic cell death in dopaminergic neuronal cells during pesticide exposures: Relevance to environmental factors and Parkinson's disease. Neurotoxicology. 2003; 24:291–292.

Kanthasamy A, Anantharam V, Ali SF, Kanthasamy AG. Methamphetamine induces autophagy and apoptosis in a mesencephalic dopaminergic neuronal culture model: role of cathepsin-D in methamphetamine-induced apoptotic cell death. Ann N Y Acad Sci. 2006; 1074:234–244. [PubMed: 17105920]

Kanthasamy A, Jin H, Mehrotra S, Mishra R, Rana A. Novel cell death signaling pathways in neurotoxicity models of dopaminergic degeneration: relevance to oxidative stress and neuroinflammation in Parkinson's disease. Neurotoxicology. 2010; 31:555–561. [PubMed: 20005250]

Kanthasamy A, Kitazawa M, Kaul S, Anantharam V, Kanthasamy AG. A novel oxidative stress-dependent apoptotic pathway in pesticide-induced dopaminergic degeneration: relevance to environmental factors and Parkinson's disease. J Neurochem. 2002; 81 suppl:76.

Kanthasamy AG, Kitazawa M, Kanthasamy A, Anantharam V. Role of proteolytic activation of protein kinase C delta in oxidative stress-induced apoptosis. Antioxidants & Redox Signaling. 2003a; 5:609–620. [PubMed: 14580317]

Kanthasamy AG, Kitazawa M, Kanthasamy A, Anantharam V. Dieldrin-induced neurotoxicity: relevance to Parkinson's disease pathogenesis. Neurotoxicology. 2005; 26:701–719. [PubMed: 16112328]

Kanthasamy AG, Kitazawa M, Kaul S, Yang Y, Lahiri DK, Anantharam V, Kanthasamy A. Proteolytic activation of proapoptotic kinase PKCdelta is regulated by overexpression of Bcl-2:

implications for oxidative stress and environmental factors in Parkinson's disease. Ann N Y Acad Sci. 2003b; 1010:683–686. [PubMed: 15033812]

Kaul S, Ananrharam V, Kanthasamy A. Low dose oxidative insult promotes apoptosis in dopaminergic cells via caspase-3 dependent proteolytic activation of PKC delta: Relevance to environmental factors and Parkinson's disease. Toxicological Sciences. 2003a; 72 79-79.

Kaul S, Anantharam V, Yang Y, Choi CJ, Kanthasamy A, Kanthasamy AG. Tyrosine phosphorylation regulates the proteolytic activation of protein kinase Cdelta in dopaminergic neuronal cells. J Biol Chem. 2005; 280:28721–28730. [PubMed: 15961393]

Kaul S, Kanthasamy A, Kitazawa M, Anantharam V, Kanthasamy AG. Caspase-3 dependent proteolytic activation of protein kinase C delta mediates and regulates 1-methyl-4-phenylpyridinium (MPP+)-induced apoptotic cell death in dopaminergic cells: relevance to oxidative stress in dopaminergic degeneration. Eur J Neurosci. 2003b; 18:1387–1401. [PubMed: 14511319]

Kitazawa M, Anantharam V, Kanthasamy A, Kanthasamy AG. Dieldrin promotes proteolytic cleavage of poly(ADP-ribose) polymerase and apoptosis in dopaminergic cells: protective effect of mitochondrial anti-apoptotic protein Bcl-2. Neurotoxicology. 2004; 25:589–598. [PubMed: 15183012]

Kitazawa, M.; Anantharam, V.; Kanthasamy, AG. Activation of oxidative stress-dependent cell signaling pathways in methylcyclopentadienyl manganese tricarbonyl (MMT)-induced apoptosis: Downstream events and regulatory mechanisms. 40th annual meeting of Society of Toxicology; 2001a.

Kitazawa M, Anantharam V, Kanthasamy AG. Dieldrin-induced oxidative stress and neurochemical changes contribute to apoptopic cell death in dopaminergic cells. Free Radic Biol Med. 2001b; 31:1473–1485. [PubMed: 11728820]

Kitazawa M, Anantharam V, Kanthasamy AG. Translocation of protein kinase CS to mitochondria promotes proteolytic inactivation of Bcl-2 during MMT-induced apoptosis in dopaminergic cells. Neurotoxicology. 2003; 24:305–306.

Kitazawa M, Anantharam V, Yang Y, Hirata Y, Kanthasamy A, Kanthasamy AG. Activation of protein kinase C delta by proteolytic cleavage contributes to manganese-induced apoptosis in dopaminergic cells: protective role of Bcl-2. Biochem Pharmacol. 2005; 69:133–146. [PubMed: 15588722]

Kitazawa M, Wagner JR, Kirby ML, Anantharam V, Kanthasamy AG. Oxidative stress and mitochondrial-mediated apoptosis in dopaminergic cells exposed to methylcyclopentadienyl manganese tricarbonyl. J Pharmacol Exp Ther. 2002; 302:26–35. [PubMed: 12065696]

Klionsky DJ, Abeliovich H, Agostinis P, Agrawal DK, Aliev G, Askew DS, Baba M, Baehrecke EH, Bahr BA, Ballabio A, Bamber BA, Bassham DC, Bergamini E, Bi X, Biard-Piechaczyk M, Blum JS, Bredesen DE, Brodsky JL, Brumell JH, Brunk UT, Bursch W, Camougrand N, Cebollero E, Cecconi F, Chen Y, Chin LS, Choi A, Chu CT, Chung J, Clarke PG, Clark RS, Clarke SG, Clave C, Cleveland JL, Codogno P, Colombo MI, Coto-Montes A, Cregg JM, Cuervo AM, Debnath J, Demarchi F, Dennis PB, Dennis PA, Deretic V, Devenish RJ, Di Sano F, Dice JF, Difiglia M, Dinesh-Kumar S, Distelhorst CW, Djavaheri-Mergny M, Dorsey FC, Droge W, Dron M, Dunn WA Jr, Duszenko M, Eissa NT, Elazar Z, Esclatine A, Eskelinen EL, Fesus L, Finley KD, Fuentes JM, Fueyo J, Fujisaki K, Galliot B, Gao FB, Gewirtz DA, Gibson SB, Gohla A, Goldberg AL, Gonzalez R, Gonzalez-Estevez C, Gorski S, Gottlieb RA, Haussinger D, He YW, Heidenreich K, Hill JA, Hoyer-Hansen M, Hu X, Huang WP, Iwasaki A, Jaattela M, Jackson WT, Jiang X, Jin S, Johansen T, Jung JU, Kadowaki M, Kang C, Kelekar A, Kessel DH, Kiel JA, Kim HP, Kimchi A, Kinsella TJ, Kiselyov K, Kitamoto K, Knecht E, et al. Guidelines for the use and interpretation of assays for monitoring autophagy in higher eukaryotes. Autophagy. 2008; 4:151–175. [PubMed: 18188003]

Kokoszka JE, Coskun P, Esposito LA, Wallace DC. Increased mitochondrial oxidative stress in the Sod2 (+/−) mouse results in the age-related decline of mitochondrial function culminating in increased apoptosis. Proc Natl Acad Sci U S A. 2001; 98:2278–2283. [PubMed: 11226230]

Konishi H, Tanaka M, Takemura Y, Matsuzaki H, Ono Y, Kikkawa U, Nishizuka Y. Activation of protein kinase C by tyrosine phosphorylation in response to H2O2. Proc Natl Acad Sci U S A. 1997; 94:11233–11237. [PubMed: 9326592]

Lam CW, James JT, McCluskey R, Hunter RL. Pulmonary toxicity of single-wall carbon nanotubes in mice 7 and 90 days after intratracheal instillation. Toxicol Sci. 2004; 77:126–134. [PubMed: 14514958]

Latchoumycandane C, Anantharam V, Kitazawa M, Yang Y, Kanthasamy A, Kanthasamy AG. Protein kinase Cdelta is a key downstream mediator of manganese-induced apoptosis in dopaminergic neuronal cells. J Pharmacol Exp Ther. 2005; 313:46–55. [PubMed: 15608081]

Lloyd RV. Mechanism of the manganese-catalyzed autoxidation of dopamine. Chem Res Toxicol. 1995; 8:111–116. [PubMed: 7703354]

Maiuri MC, Le Toumelin G, Criollo A, Rain JC, Gautier F, Juin P, Tasdemir E, Pierron G, Troulinaki K, Tavernarakis N, Hickman JA, Geneste O, Kroemer G. Functional and physical interaction between Bcl-X(L) and a BH3-like domain in Beclin-1. Embo J. 2007a; 26:2527–2539. [PubMed: 17446862]

Maiuri MC, Zalckvar E, Kimchi A, Kroemer G. Self-eating and self-killing: crosstalk between autophagy and apoptosis. Nat Rev Mol Cell Biol. 2007b; 8:741–752. [PubMed: 17717517]

Mao H, Fang X, Floyd KM, Polcz JE, Zhang P, Liu B. Induction of microglial reactive oxygen species production by the organochlorinated pesticide dieldrin. Brain Res. 2007; 1186:267–274. [PubMed: 17999924]

Marquis BJ, Love SA, Braun KL, Haynes CL. Analytical methods to assess nanoparticle toxicity. Analyst. 2009; 134:425–439. [PubMed: 19238274]

Miranda M, Sorkina T, Grammatopoulos TN, Zawada WM, Sorkin A. Multiple molecular determinants in the carboxyl terminus regulate dopamine transporter export from endoplasmic reticulum. J Biol Chem. 2004; 279:30760–30770. [PubMed: 15128747]

Mizushima N, Yoshimori T. How to interpret LC3 immunoblotting. Autophagy. 2007; 3:542–545. [PubMed: 17611390]

Mizushima N, Yoshimori T, Levine B. Methods in mammalian autophagy research. Cell. 2010; 140:313–326. [PubMed: 20144757]

Monteiro-Riviere NA, Nemanich RJ, Inman AO, Wang YY, Riviere JE. Multi-walled carbon nanotube interactions with human epidermal keratinocytes. Toxicol Lett. 2005; 155:377–384. [PubMed: 15649621]

Mukhopadhyay P, Rajesh M, Yoshihiro K, Hasko G, Pacher P. Simple quantitative detection of mitochondrial superoxide production in live cells. Biochem Biophys Res Commun. 2007; 358:203–208. [PubMed: 17475217]

Nel A, Xia T, Madler L, Li N. Toxic potential of materials at the nanolevel. Science. 2006; 311:622–627. [PubMed: 16456071]

Oberdorster E. Manufactured nanomaterials (fullerenes, C60) induce oxidative stress in the brain of juvenile largemouth bass. Environ Health Perspect. 2004; 112:1058–1062. [PubMed: 15238277]

Oberdorster G, Gelein RM, Ferin J, Weiss B. Association of particulate air pollution and acute mortality: involvement of ultrafine particles? Inhal Toxicol. 1995; 7:111–124. [PubMed: 11541043]

Oberdorster G, Oberdorster E, Oberdorster J. Nanotoxicology: An emerging discipline evolving from studies of ultrafine particles. Environmental Health Perspectives. 2005; 113:823–839. [PubMed: 16002369]

Olanow CW. Manganese-induced parkinsonism and Parkinson's disease. Ann N Y Acad Sci. 2004; 1012:209–223. [PubMed: 15105268]

Oztap E, Topal A. A cell protective mechanism in a murine model of Parkinson’s disease. Turk J Med Sci. 2003; 33:295–299.

Park RM, Bowler RM, Eggerth DE, Diamond E, Spencer KJ, Smith D, Gwiazda R. Issues in neurological risk assessment for occupational exposures: the Bay Bridge welders. Neurotoxicology. 2006; 27:373–384. [PubMed: 16332392]

Pattingre S, Tassa A, Qu X, Garuti R, Liang XH, Mizushima N, Packer M, Schneider MD, Levine B. Bcl-2 antiapoptotic proteins inhibit Beclin 1-dependent autophagy. Cell. 2005; 122:927–939. [PubMed: 16179260]

Peng X, Tehranian R, Dietrich P, Stefanis L, Perez RG. Alpha-synuclein activation of protein phosphatase 2A reduces tyrosine hydroxylase phosphorylation in dopaminergic cells. J Cell Sci. 2005; 118:3523–3530. [PubMed: 16030137]

Segura-Aguilar J, Lind C. On the mechanism of the Mn3(+)-induced neurotoxicity of dopamine:prevention of quinone-derived oxygen toxicity by DT diaphorase and superoxide dismutase. Chem Biol Interact. 1989; 72:309–324. [PubMed: 2557982]

Song C, Kanthasamy A, Anantharam V, Sun F, Kanthasamy AG. Environmental neurotoxic pesticide increases histone acetylation to promote apoptosis in dopaminergic neuronal cells: relevance to epigenetic mechanisms of neurodegeneration. Mol Pharmacol. 2010; 77:621–632. [PubMed: 20097775]

Sun F, Anantharam V, Zhang D, Latchoumycandane C, Kanthasamy A, Kanthasamy AG. Proteasome inhibitor MG-132 induces dopaminergic degeneration in cell culture and animal models. Neurotoxicology. 2006; 27:807–815. [PubMed: 16870259]

Sun W, Fang N, Trewyn BG, Tsunoda M, Slowing II, Lin VSY, Yeung ES. Endocytosis of a single mesoporous silica nanoparticle into a human lung cancer cell observed by differential interference contrast microscopy. Analytical and Bioanalytical Chemistry. 2008; 391:2119–2125. [PubMed: 18488205]

Tanida I, Ueno T, Kominami E. LC3 and Autophagy. Methods Mol Biol. 2008; 445:77–88. [PubMed: 18425443]

Technology T.P.s. C. o. A. o. S. a. The National Nanotechnology Initiative 2010. Third Assessment along with Recommendations of the National Nanotechnology Advisory Panel. Washington, D.C: Executive Office of the President President's Council of Advisors on Science and Technology; 2010. Report To The President And Congress On The Third Assessment Of The National Nanotechnology Initiative; p. 1-96.

Teeguarden JG, Hinderliter PM, Orr G, Thrall BD, Pounds JG. Particokinetics in vitro: Dosimetry considerations for in vitro nanoparticle toxicity assessments. Toxicological Sciences. 2007; 95:300–312. [PubMed: 17098817]

Thomas K, Sayre P. Research strategies for safety evaluation of nanomaterials, Part I: evaluating the human health implications of exposure to nanoscale materials. Toxicol Sci. 2005; 87:316–321. [PubMed: 16049265]

Thomas T, Thomas K, Sadrieh N, Savage N, Adair P, Bronaugh R. Research strategies for safety evaluation of nanomaterials, part VII: evaluating consumer exposure to nanoscale materials. Toxicol Sci. 2006; 91:14–19. [PubMed: 16476686]

Toh TB, Chen MJ, Armugam A, Peng ZF, Li QT, Jeyaseelan K, Cheung NS. Antioxidants: promising neuroprotection against cardiotoxin-4b-induced cell death which triggers oxidative stress with early calpain activation. Toxicon. 2008; 51:964–973. [PubMed: 18377942]

Tsuji JS, Maynard AD, Howard PC, James JT, Lam CW, Warheit DB, Santamaria AB. Research strategies for safety evaluation of nanomaterials, part IV: risk assessment of nanoparticles. Toxicol Sci. 2006; 89:42–50. [PubMed: 16177233]

Warheit DB, Borm PJ, Hennes C, Lademann J. Testing strategies to establish the safety of nanomaterials: conclusions of an ECETOC workshop. Inhal Toxicol. 2007; 19:631–643. [PubMed: 17510836]

Wirawan E, Vande Walle L, Kersse K, Cornelis S, Claerhout S, Vanoverberghe I, Roelandt R, De Rycke R, Verspurten J, Declercq W, Agostinis P, Vanden Berghe T, Lippens S, Vandenabeele P. Caspase-mediated cleavage of Beclin-1 inactivates Beclin-1-induced autophagy and enhances apoptosis by promoting the release of proapoptotic factors from mitochondria. Cell Death and Disease. 2010; 1:e18. 10.1038/cddis.2009.1016. [PubMed: 21364619]

Wu X, Bruchez MP. Labeling cellular targets with semiconductor quantum dot conjugates. Methods Cell Biol. 2004; 75:171–183. [PubMed: 15603426]

Yang Y, Kaul S, Zhang D, Anantharam V, Kanthasamy AG. Suppression of caspase-3-dependent proteolytic activation of protein kinase C delta by small interfering RNA prevents MPP+-induced dopaminergic degeneration. Mol Cell Neurosci. 2004; 25:406–421. [PubMed: 15033169]

Zhang D, Kanthasamy A, Anantharam V. Effects of manganese on tyrosine hydroxylase (TH) activity and TH-phosphorylation in a dopaminergic neural cell line. Toxicol Appl Pharmacol. 2011

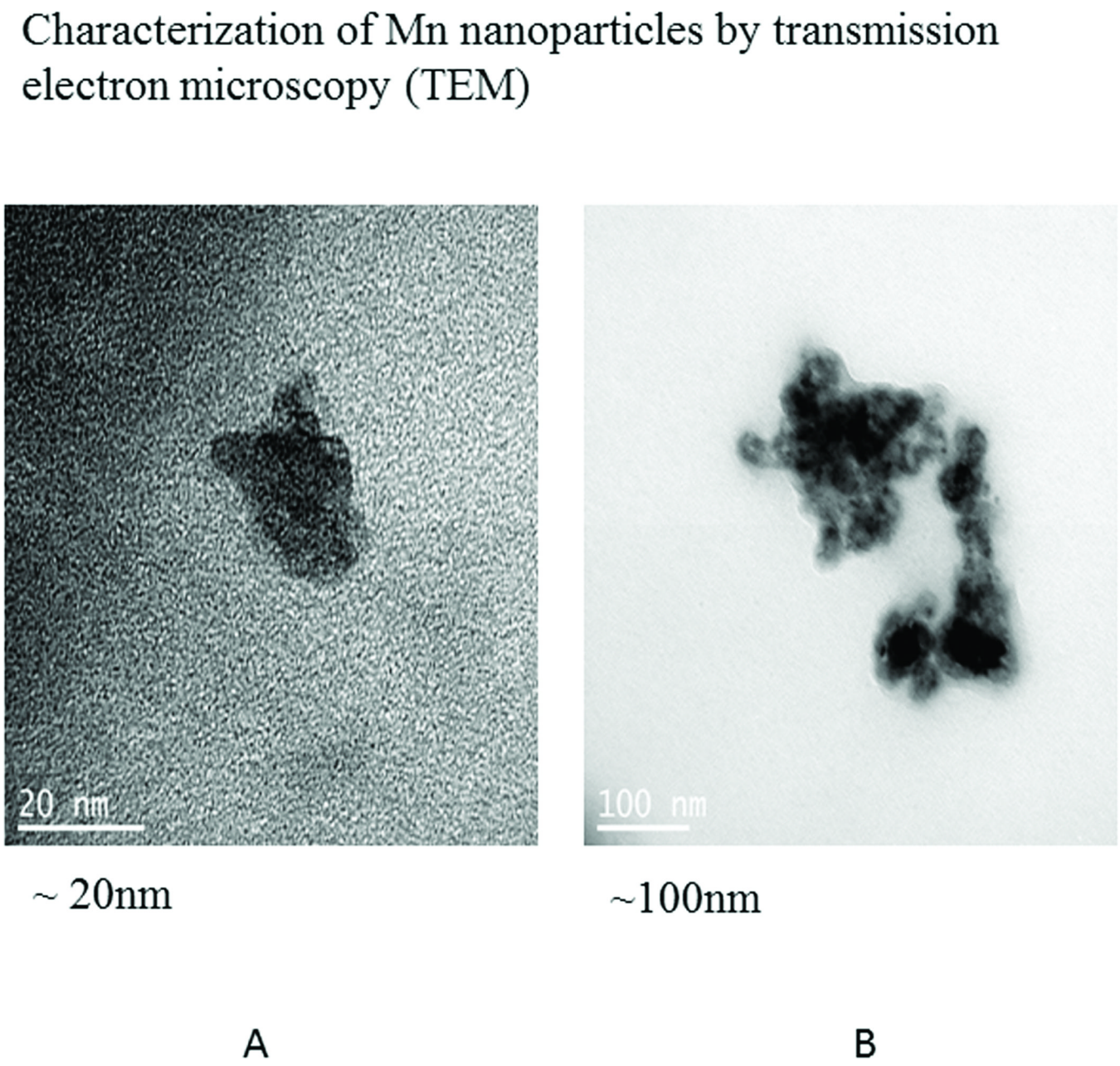

Fig. 1.

Transmission electron microscopy (TEM) of Mn nanoparticles. Mn nanoparticles were a black powder that tended to agglomerate in solution. Mn nanoparticle dispersion in RPMI was observed with advanced high-illuminating TEM microscopy. Dispersed nanoparticles (20 mg/mL) suspended in 10% supplemented RPMI cell culture media occur as: (A) Single Mn nanoparticles and (B) Agglomerated Mn nanoparticles.

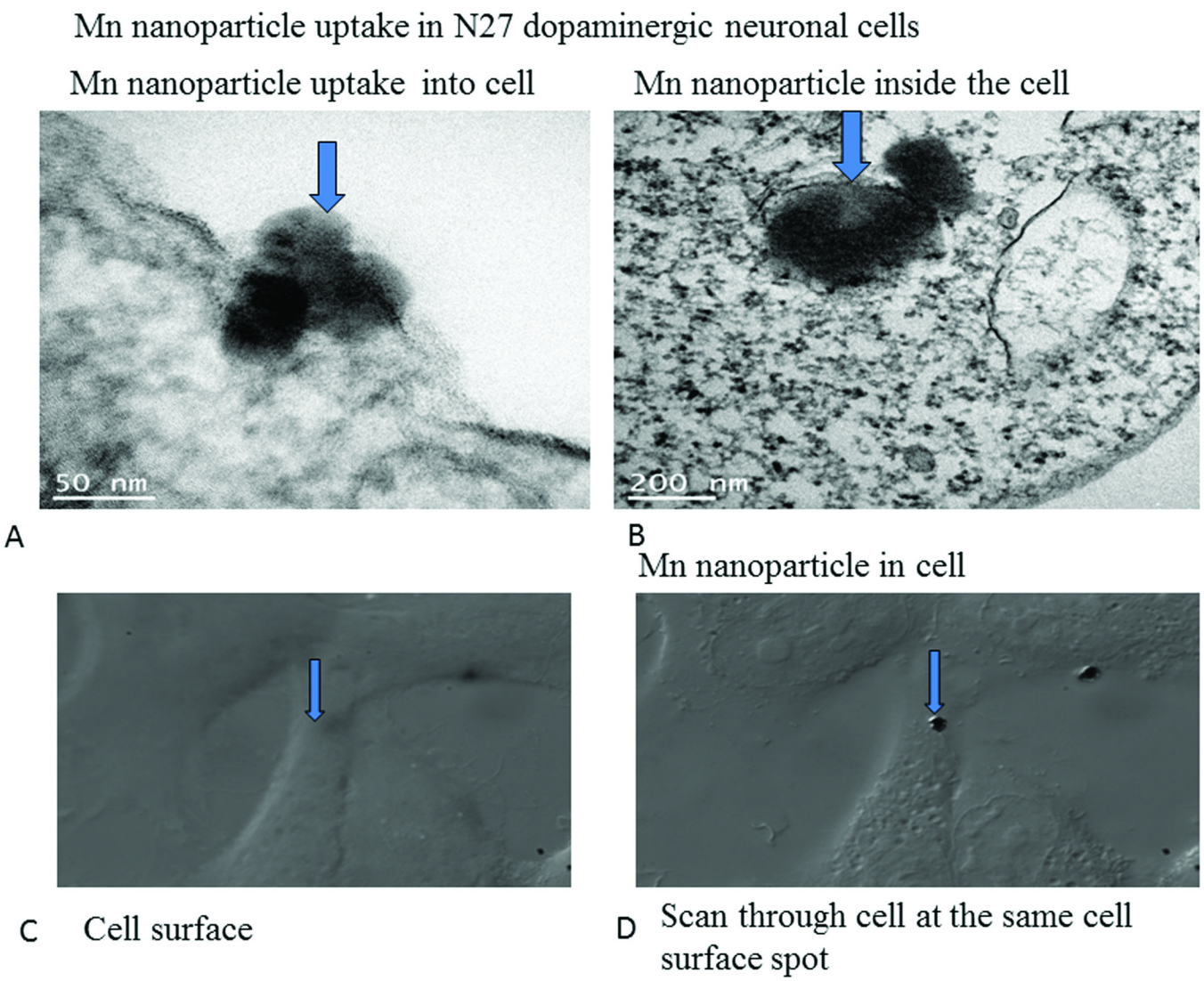

Fig. 2.

Uptake of Mn nanoparticles viewed with TEM and DIC microscopy. Mn nanoparticle uptake was visualized after N27 dopaminergic cells were exposed to 50 μg/mL Mn nanoparticles for up to 6 h. When visualized with TEM, nanoparticles (~50 nm) can be seen on the cell membrane (A) in the early phases of internalization and inside the cytoplasm (B) following internalization. The internalization of Mn nanoparticles was also evident when viewed with a DIC microscope, as shown in (C) Mn nanoparticle on the cell surface of N27 cell, and (D) one of the imaged layers below the cell surface. Data represent results from at least four individual measurements.

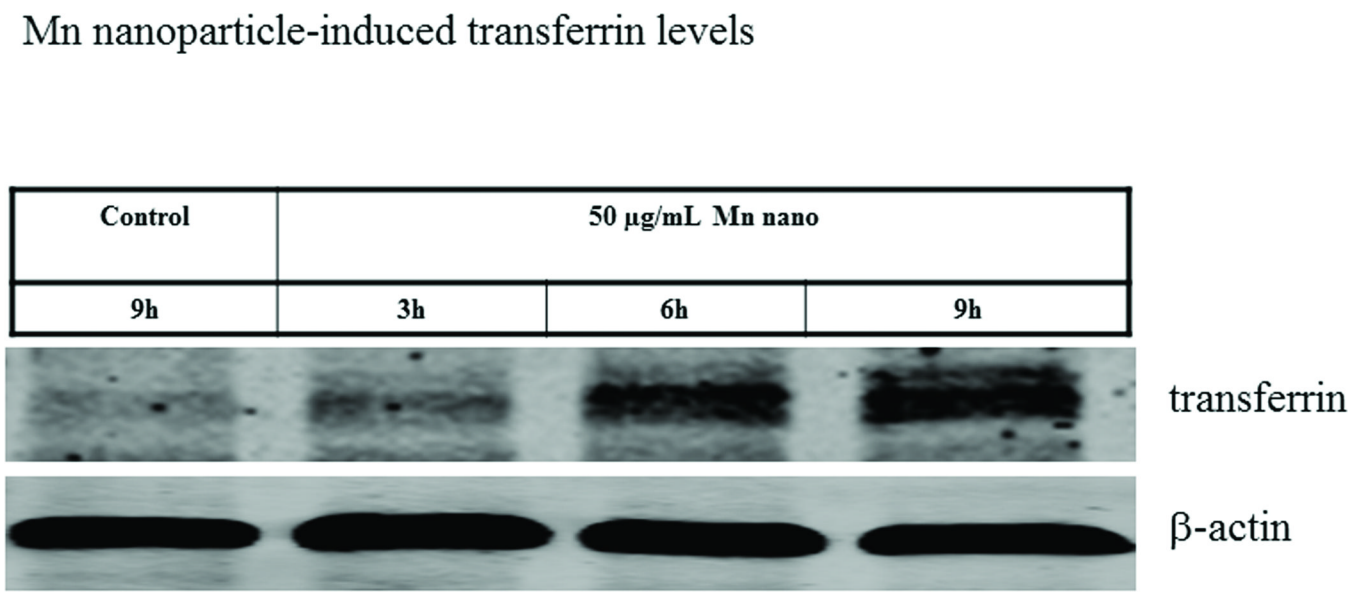

Fig. 3.

Mn nanoparticles induce a dose- and time-dependent neurotoxic effect on N27 dopaminergic neuronal cells. The effect of Mn nanoparticles on cell viability in N27 dopaminergic neuronal cells. (A) Quantitative analysis of dose-dependent Mn nanoparticle-induced neurotoxicity was measured by the Sytox green cytotoxicity fluorescence assay. The cells were exposed to 0–400 µg/mL Mn nanoparticles for 6 h and then neurotoxicity was measured using the Sytox green fluorescence assay. (B) Quantitative analysis of time-dependent Mn nanoparticle-induced neurotoxicity was measured by the Sytox green cytotoxicity fluorescence assay. The cells were exposed to 50 µg/mL Mn nanoparticles for 3, 6 and 9 h and then neurotoxicity was measured using the Sytox green fluorescence assay. The Sytox fluorescence was measured using a BioTek fluorescence microplate reader. Data represent results from at least eight individual measurements and are expressed as mean ± S.E.M. $P< 0.01$ **, $P< 0.001$***, $P< 0.001$ # between control and treatment at the same time point. (C) Visualization of Mn nanoparticle-induced neurotoxicity by Sytox green fluorescence assay. N27 dopaminergic neuronal cells were exposed to 50 µg/mL Mn nanoparticles for 9 h and then cells were loaded with Sytox green and observed under a Nikon inverted fluorescence microscope and pictures were captured with a SPOT digital camera (Diagnostic Instruments, Sterling Heights, MI).

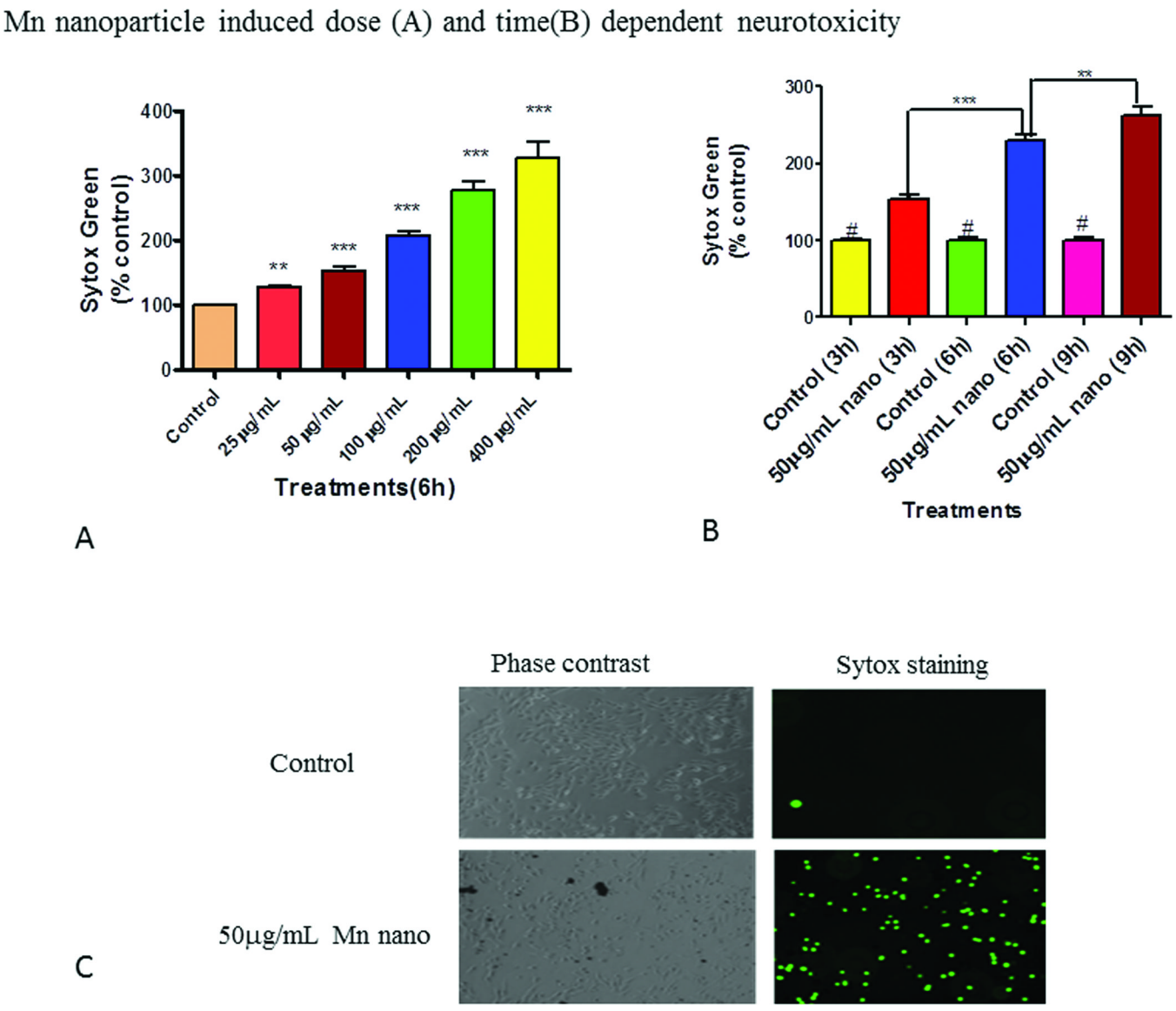

Fig. 4.

Time-dependent upregulation of Transferrin (Tf). N27 cells were treated with 50 µg/mL Mn nanoparticles for 3, 6 and 9 h and then a Tf immunoblot was performed, as described in the methods. To confirm equal protein loading in each lane, the membranes were reprobed with β-actin antibody. Data represent results from at least three separate experiments.

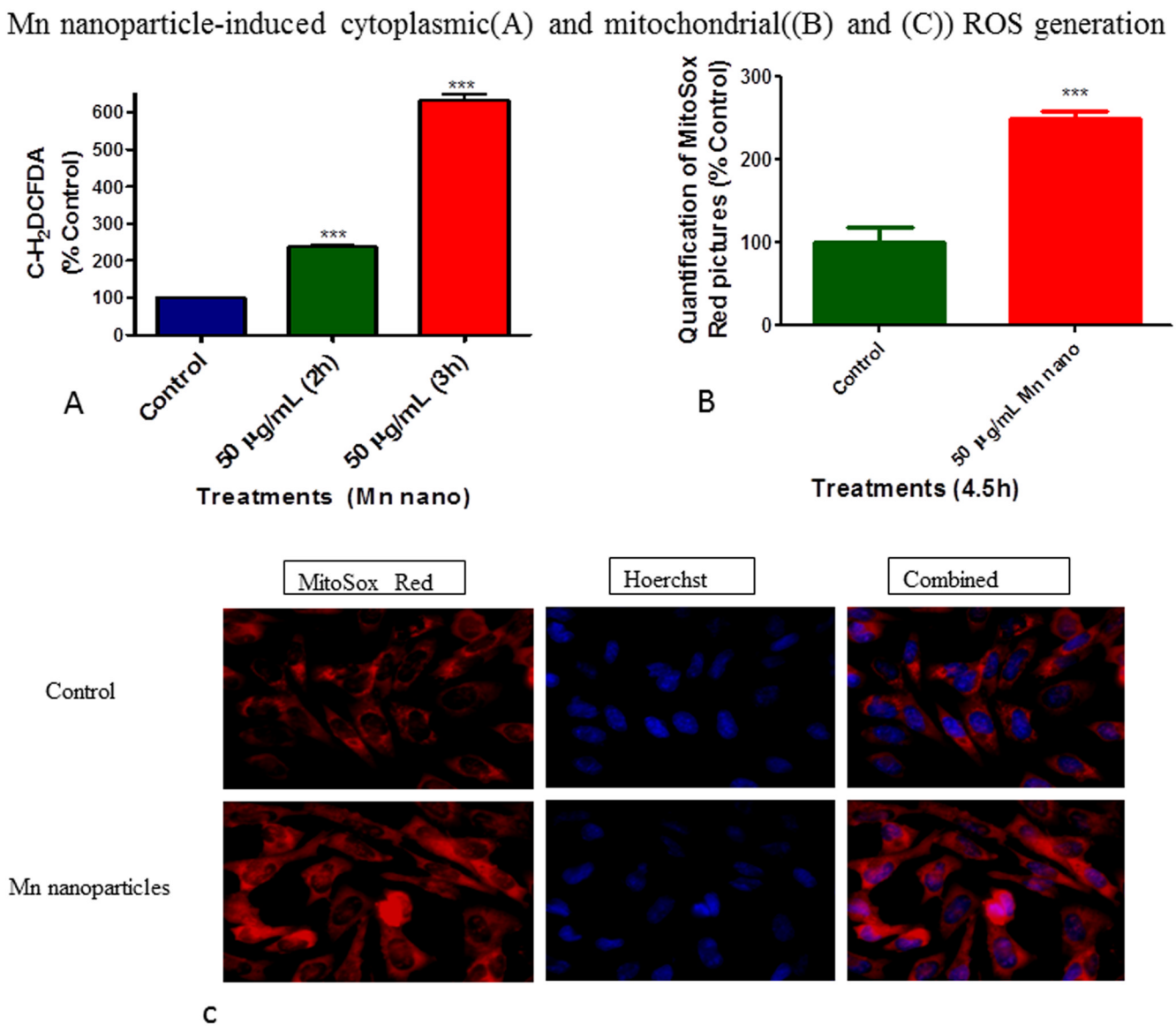

Fig. 5.

Mn nanoparticle-induced ROS generation in N27 dopaminergic neuronal cells. (A) Mn nanoparticles induced a time-dependent cytoplasmic H_2O_2 generation in N27 cells. The measurements were conducted in a 96 well plate containing the cells exposed to 50 µg/mL Mn nanoparticles for up to 3 h. Reactive oxygen species (ROS) generation/production was measured after washing the treated cells with HBSS, followed by a 15–20 minute incubation in 10 µM H_2DCF-DA. DCF-DA fluorescence was measured using a Bio-Tek fluorescence microplate reader at excitation wavelength of 485 nm and emission wavelength of 535 nm. Data represent results from at least eight individual measurements and are expressed as mean ± S.E.M. P< 0.001*** between control and treatment. (B) and (C) Manganese nanoparticles increase mitochondrial superoxide formation in N27 dopaminergic neurons. Representative images (C) of N27 cells and their quantitation (B) showing increases in mitochondrial MitoSOX fluorescence following treatment with 50 µg/mL Mn nanoparticles for 4.5 h. Data represent results from at least two individual measurements.

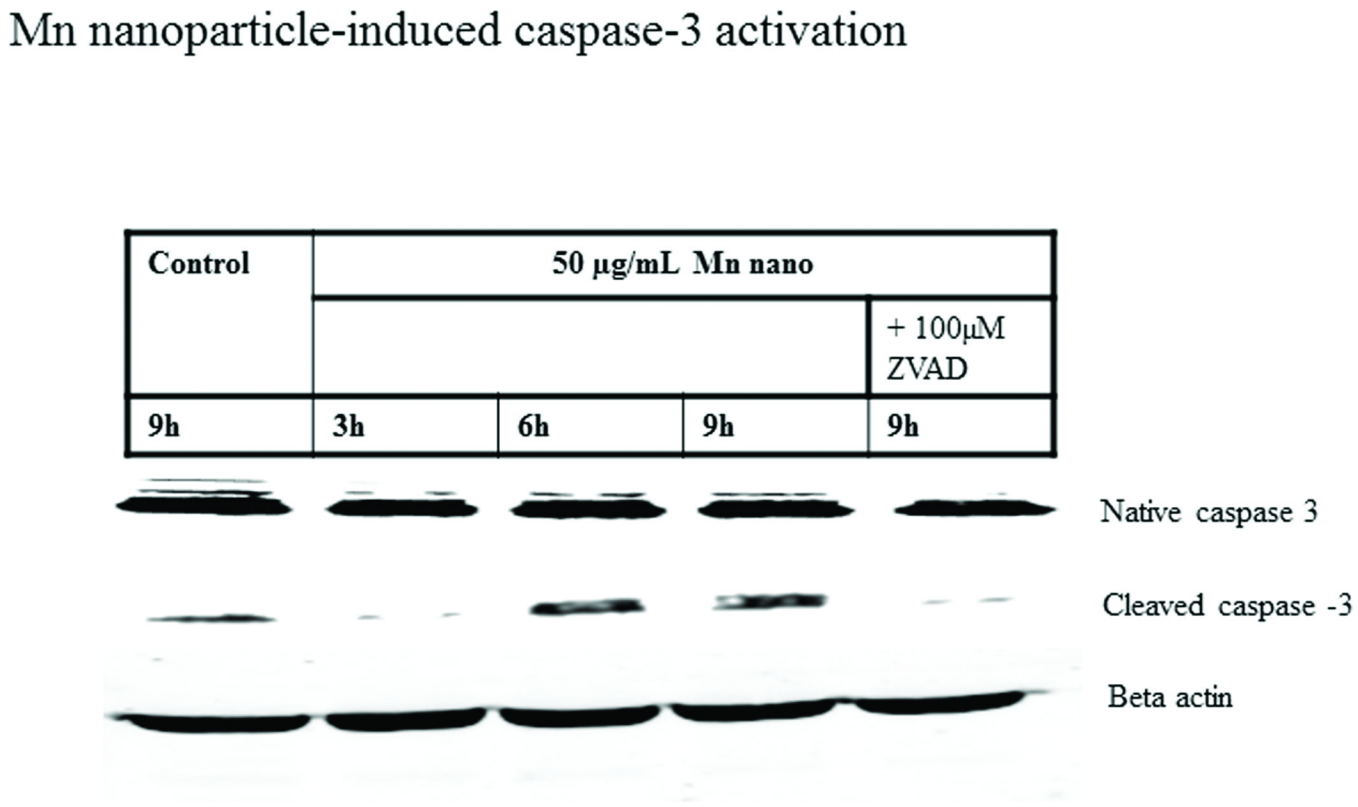

Fig. 6.

Manganese nanoparticles activate caspase-3 in N27 dopaminergic neurons by inducing caspase-3 cleavage. Caspase-3 was immunoblotted after 50 µg/mL Mn nanoparticle treatment in N27 dopaminergic neuronal cells for 3, 6 and 9 h in the presence or absence of 100 µM Z-VAD-FMK for the 9 h time point. Proteins were separated from lysates by 15% SDS-PAGE and the immunoblot was probed with caspase-3 antibody to observe both native (32 kDa) and cleaved (17 kDa) caspase-3 bands. To confirm equal protein loading in each lane, the membranes were reprobed with β-actin antibody. Data represent results from at least three individual measurements.

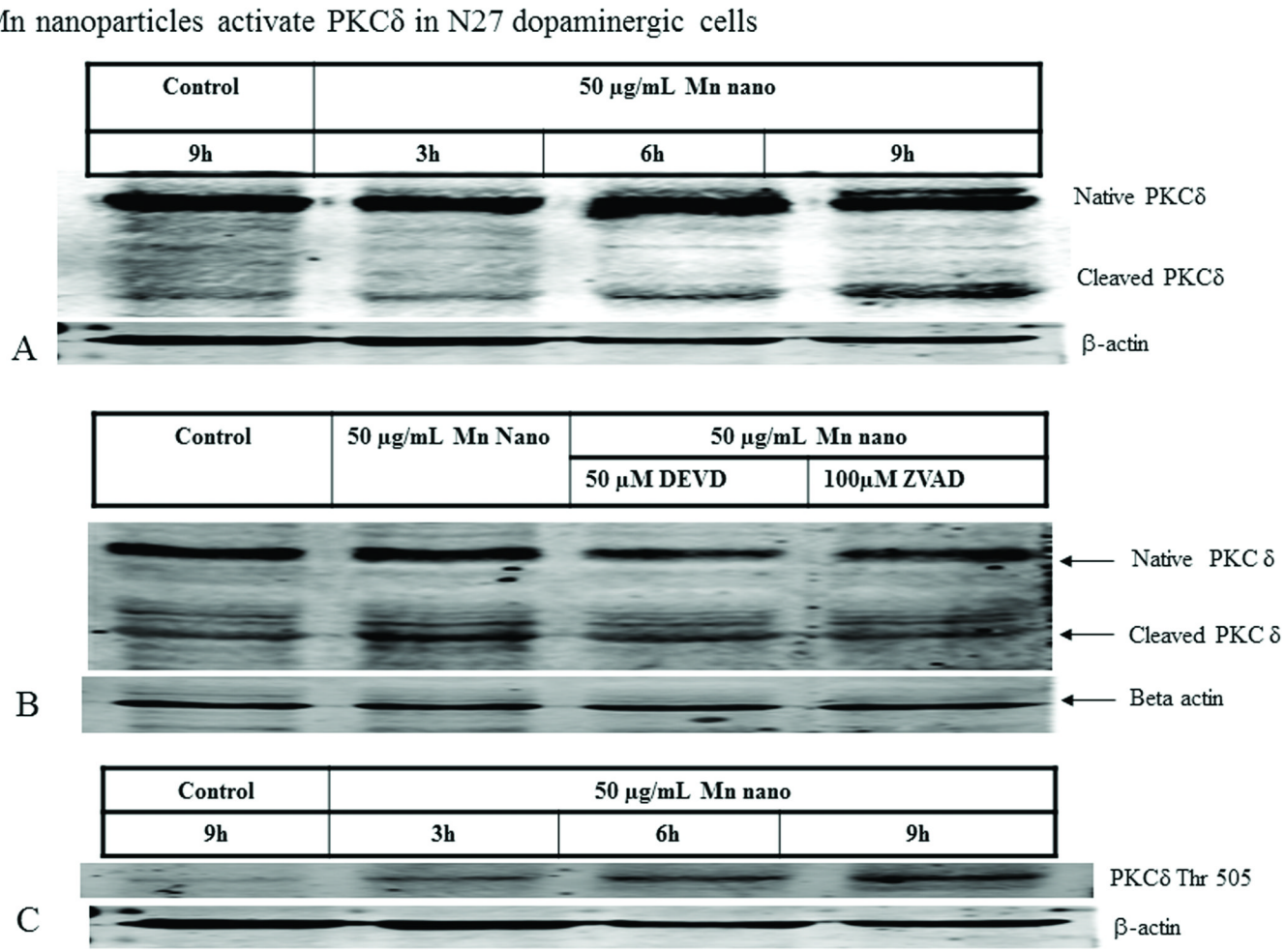

Fig. 7.

Manganese nanoparticles activate PKCδ in dopaminergic neuronal cells. N27 dopaminergic cells were treated with 50 μg/mL Mn nanoparticles for 3–9 hr. **(A)** Manganese nanoparticle-induced PKCδ cleavage and **(C)** phosphorylation of PKCδ at the Threonine 505 site were determined by Western blot. Also, 50 μg/mL Mn nanoparticle treatment for 9 h with or without a 30 min pretreatment with pan caspase inhibitor (100 μM Z-VAD-FMK) or caspase-3 specific inhibitor (100 μM Z-DEVD-FMK). **(B)** PKCδ cleavage was measured by Western blot. To confirm equal protein loading in each lane, the membranes were reprobed with β-actin antibody. Data represent results from at least three individual measurements.

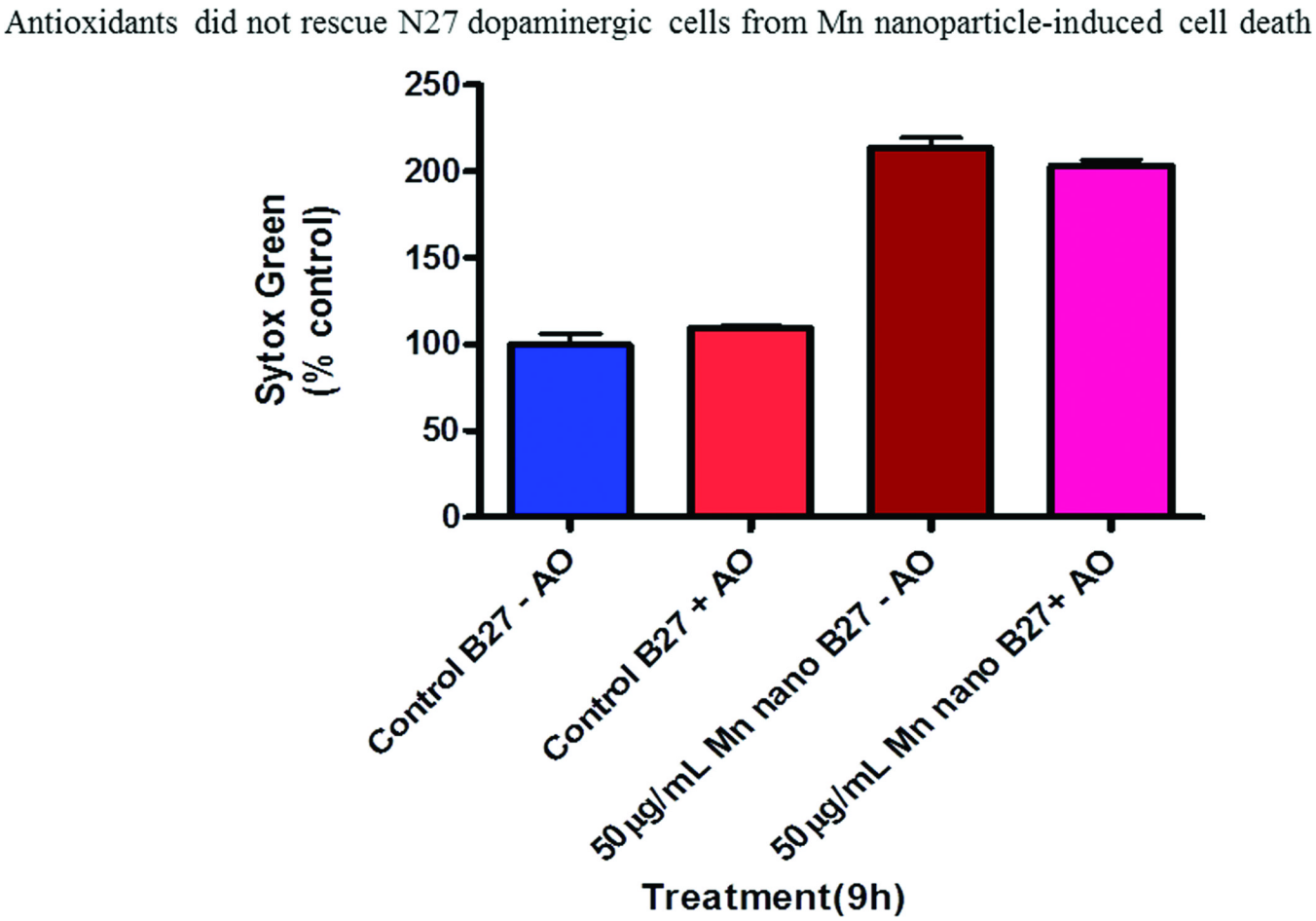

Fig. 8.

Effect of antioxidants on Mn nanoparticle-induced neurotoxicity. N27 dopaminergic neuronal cells were co-treated with 50 µg/mL Mn nanoparticles and an antioxidant solution cocktail (AO) of vitamin E, glutathione, superoxide dismutase, and catalase. A quantitative analysis showing no effect of AO on Mn nanoparticle-induced neurotoxicity was measured by the Sytox green cytotoxicity fluorescence assay. Data represent results from eight individual measurements and are expressed as mean ± S.E.M.

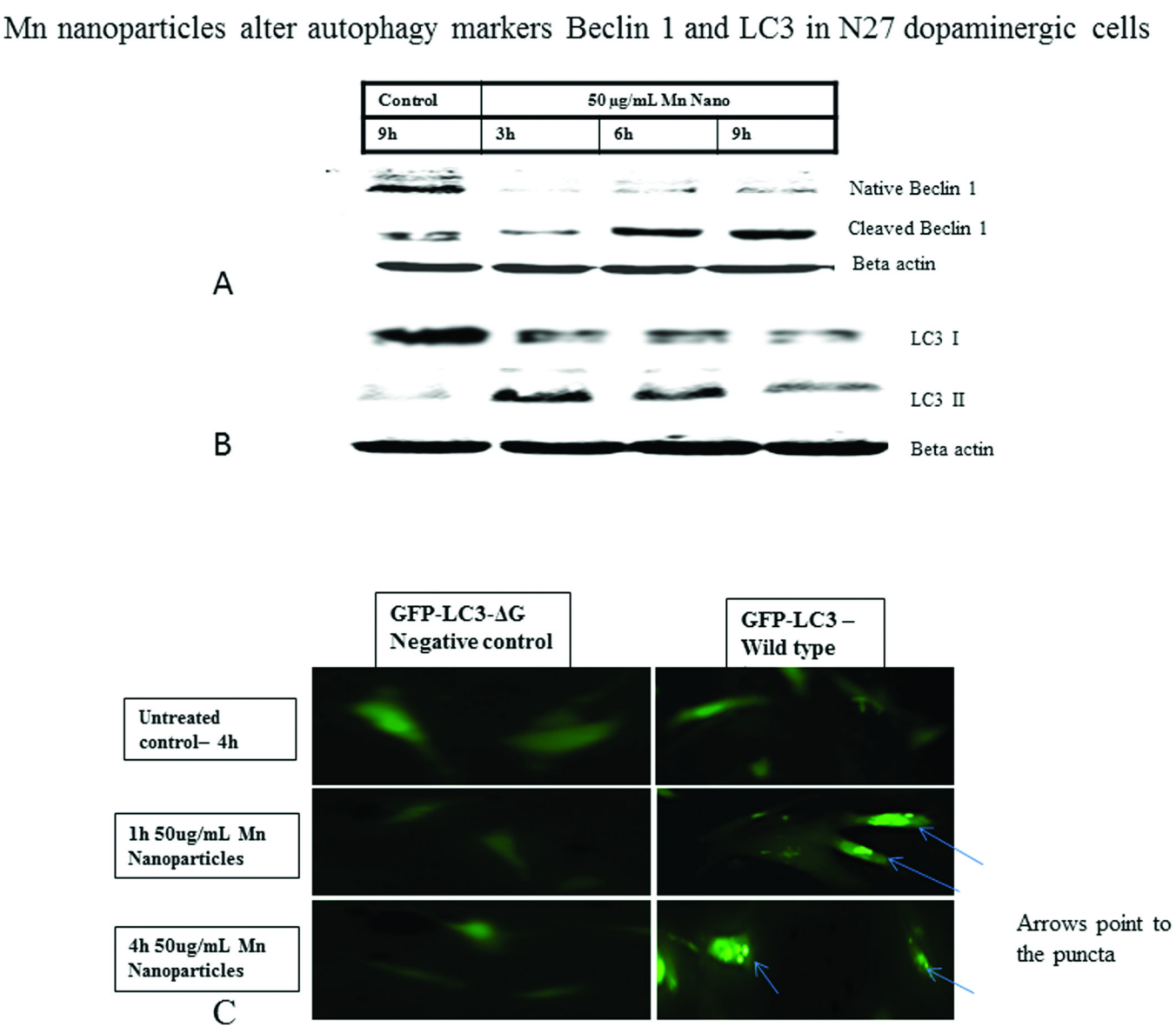

Fig. 9.

Activation of autophagy markers LC3 and Beclin-1 in Mn nanoparticle-induced neurotoxicity. **(A)** Mn nanoparticles decreased native Beclin-1 levels and induced Beclin-1 cleavage. Beclin-1 was immunoblotted after 50 μg/mL Mn nanoparticle treatment in N27 dopaminergic neuronal cells for 3, 6 and 9 h. A 10–12% SDS-PAGE was used to separate the proteins and the immunoblot was probed with Beclin-1 antibody to observe both native (60 kDa) and cleaved (37kDa) Beclin-1 bands. To confirm equal protein loading in each lane, the membranes were reprobed with β-actin antibody. Data represent results from at least three individual measurements. **(B)** Levels of autophagy marker LC3 are altered during Mn nanoparticle neurotoxicity in N27 cells. N27 cells were treated with 50 μg/mL Mn nanoparticles for 3, 6 and 9 h and then an LC3 immunoblot was performed, as described in the methods. LC3I levels decreased while LC3II levels increased. To confirm equal protein loading in each lane, the membranes were reprobed with β-actin antibody. Data represent results from at least three separate experiments. (C) N27 cells transfected with wild type GFP-LC3 form punctate as a measure of autophagy following exposure to Mn nanoparticles.

N27 cells were transiently transfected with either GFP-LC3 or GFP-LC3-ΔG, as described in the methods. Puncta was formed in cells transfected with GFP-LC3 cDNA and treated with Mn nanoparticles for 3 and 6 h. GFP-LC3 dots were not observed when cells were transfected with GFP-LC3-ΔG cDNA.

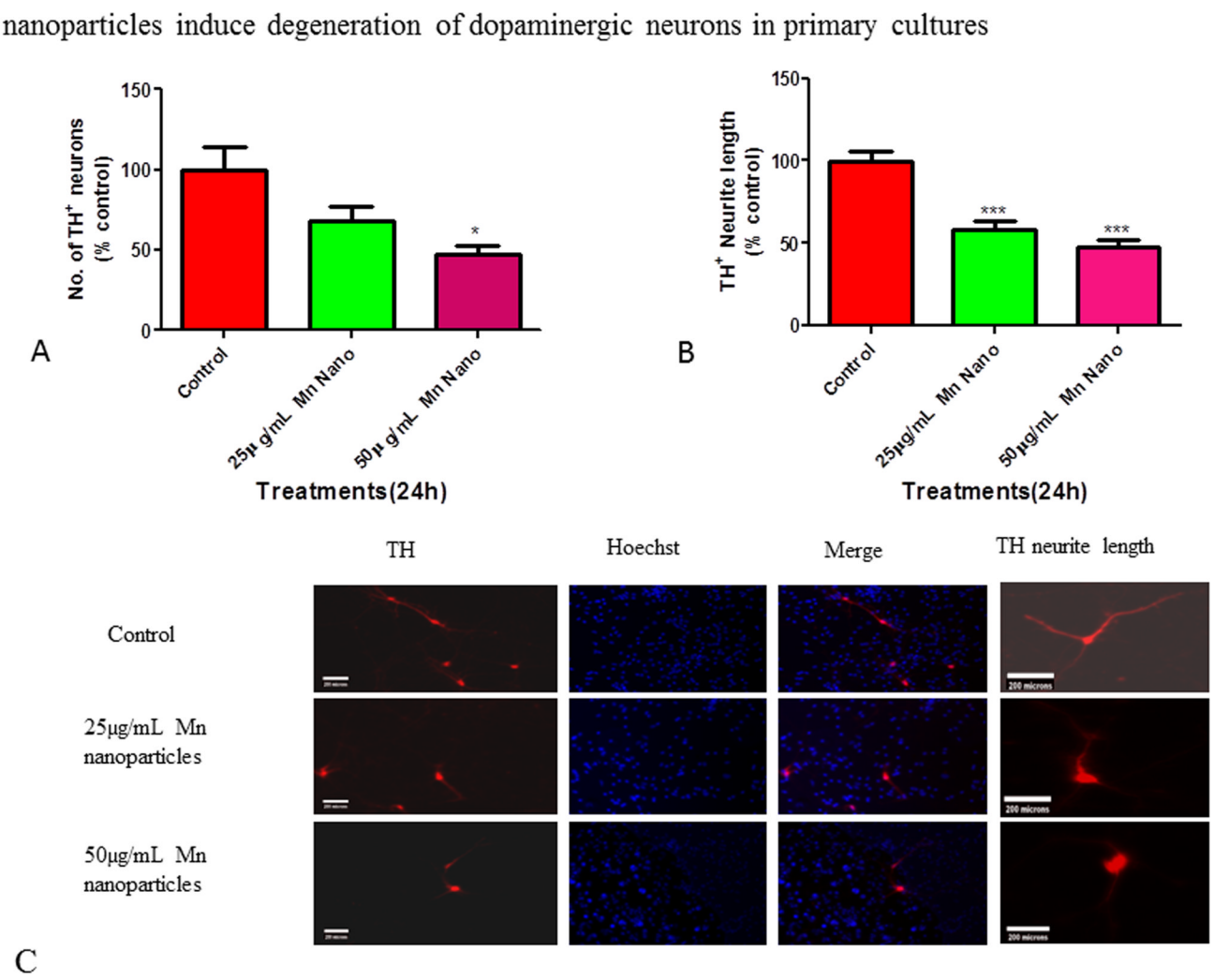

Fig. 10.

Mn nanoparticles are neurotoxic to primary nigral dopaminergic neurons. A. Mouse mesencephalic primary neurons were cultured and grown on poly-d-lysine-coated coverslips. The culture cells were exposed to 25 µg/mL Mn nanoparticles and 50 µg/mL Mn nanoparticles for 24 h, and the viability of dopaminergic neurons was measured by tyrosine hydroxylase (TH) immunohistochemistry. After treatment, the primary neurons were fixed, immunostained for TH and viewed under a Nikon TE2000 fluorescence microscope, as described in the methods. (A) TH cell count and (B) length of neuronal processes were quantified using MetaMorph image analysis software, as described in the methods. Asterisks (*, $p < 0.05$ and ***, $p < 0.001$; $n = 8$) indicate significant difference compared with control neurons. (C) Immunostained TH primary neurons showing number of TH neurons and their lengths following different treatments. The scale bar on the pictures is representative of 200 microns. The data are representative of at least 8 coverslips per treatment group.

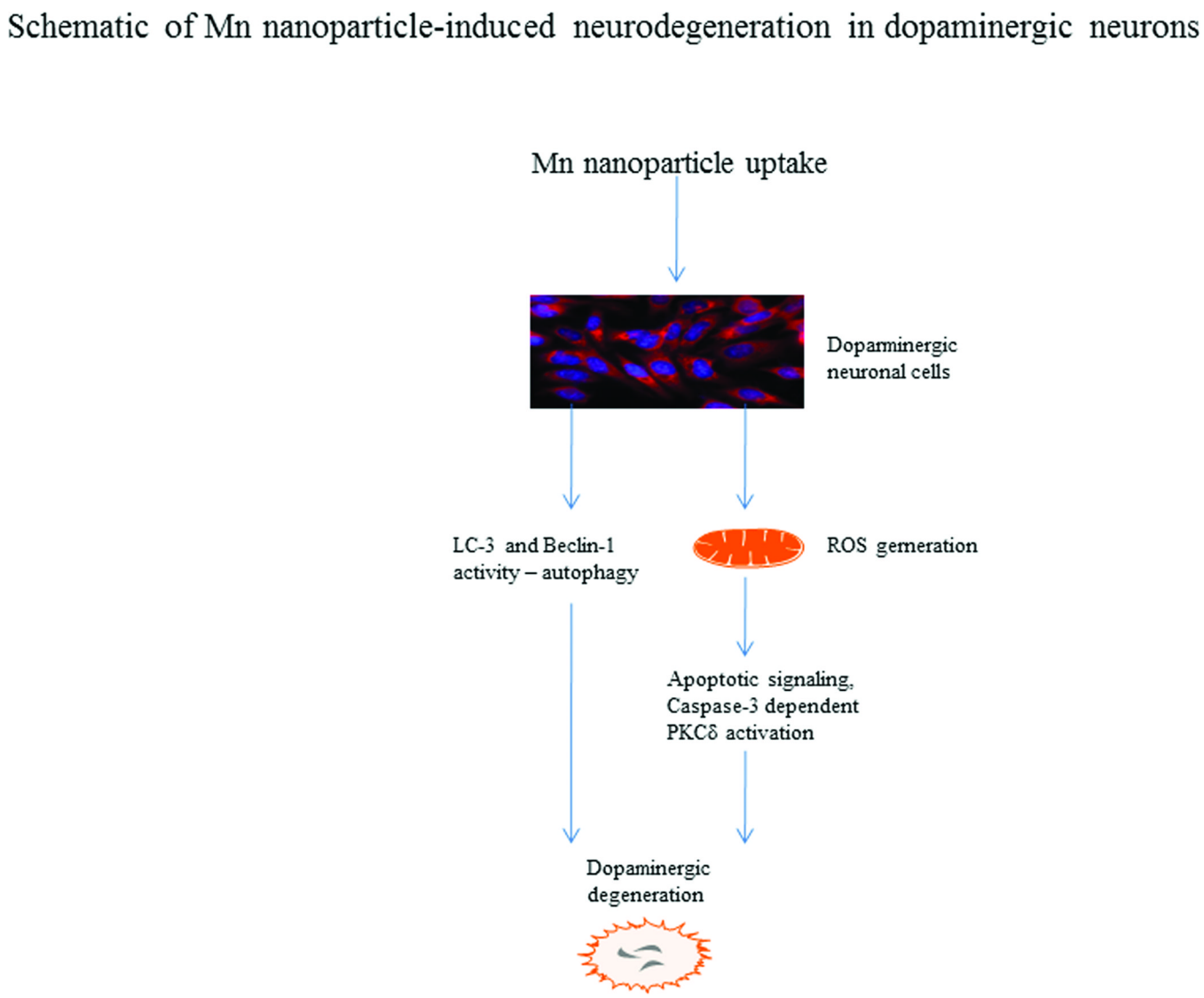

Fig. 11.
Schematic of the possible mechanisms involved in the neurotoxicity of manganese nanoparticles to dopaminergic neuronal cells.